

Electronic Supporting Information

**Dianionic Nitrogen-rich Triazole and Tetrazole-Based Energetic Salts: Synthesis and Detonation Performance**

Abhishek Kumar Yadav,<sup>a</sup> Vikas D. Ghule,<sup>b</sup> Srinivas Dharavath<sup>a\*</sup>

<sup>a</sup>Energetic Materials Laboratory, Department of Chemistry, Indian Institute of Technology Kanpur, Kanpur-208016, Uttar Pradesh, India. E-mail: [srinivasd@iitk.ac.in](mailto:srinivasd@iitk.ac.in)

<sup>b</sup>Department of Chemistry, National Institute of Technology Kurukshetra, Kurukshetra-136119, Haryana, India.

**Table of Contents**

General Methods	S2
Crystal Structure Analysis for <b>4</b> and <b>15</b>	S2-S11
Energetic data, Oxygen & Nitrogen Contents for <b>3</b> to <b>16</b>	S11
NMR Spectra, DSC plots & IR Spectrum for <b>4</b> to <b>16</b>	S12-S40
Computational	S41-S43
References	S44

**Caution!** All the compounds investigated are potentially explosive, energetic materials. Although we have experienced no difficulties in syntheses and characterization of these compounds, manipulations must be carried out by using appropriate standard safety precautions. Eye protection and leather gloves must be worn at all times.

## General Methods

All reagents were purchased from Aldrich, Merck, Alfa Aesar, or Avra in analytical grade and were used as supplied, if not stated otherwise.  $^1\text{H}$ , and  $^{13}\text{C}$  spectra were recorded on a JEOL ECS 400 MHz NMR spectrometer nuclear magnetic resonance spectrometer. Chemical shifts are reported relative to  $\text{Me}_4\text{Si}$ . The decomposition points were obtained on a  $10\text{ }^\circ\text{C min}^{-1}$ . IR spectra were recorded on an FT-IR spectrometer (Thermo Nicolet AVATAR 370) as thin films using KBr plates. Elemental analyses were determined using an Elementar vario MICRO elemental analyzer. The sensitivities were carried out by using a BAM drop hammer and friction tester.

## X-ray Crystallography

For compounds **4** and **15**, a colourless prism of dimensions  $0.600 \times 0.051 \times 0.020\text{ mm}^3$ ,  $0.600 \times 0.051 \times 0.020\text{ mm}^3$  was separately mounted on a MiteGen MicroMesh using a small amount of Cargille immersion oil for the X-ray crystallographic analysis. Data were collected on a Bruker three-circle platform diffractometer equipped with a SMART APEX II CCD detector. The crystals were irradiated using graphite monochromated  $\text{MoK}\alpha$  radiation ( $\lambda = 0.71073\text{ \AA}$ ). An Oxford Cobra low-temperature device was used to keep the crystals at a constant  $100(2)\text{ K}$  for **4** and **15** during data collection.

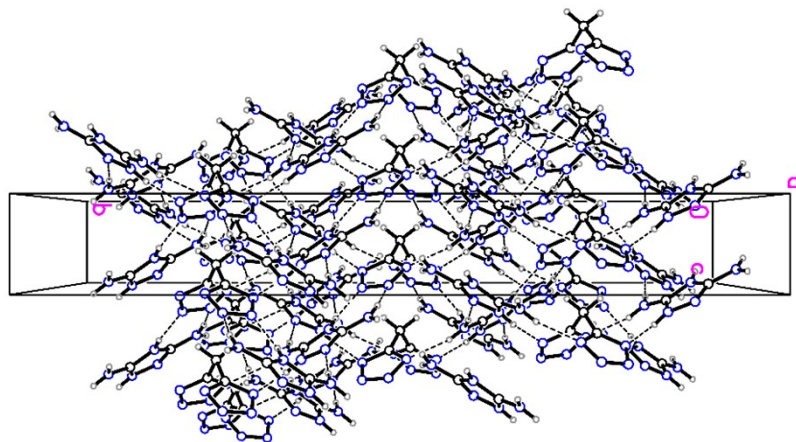
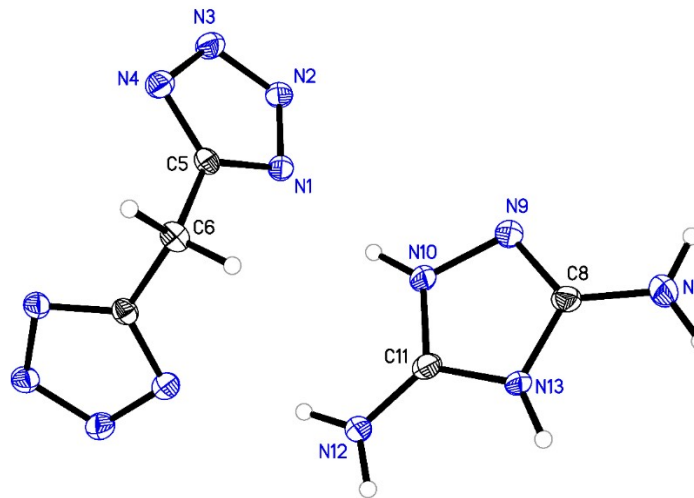


**Figure S1.** Molecular structure of **4**.

**Table S1:** Crystallographic data for **4**.

Compound	4
Formula	C <sub>7</sub> H <sub>14</sub> N <sub>18</sub>
CCDC number	2113929

Mw	350.36
Crystal size [mm3]	0.331 x 0.105 x 0.020
Crystal system	Orthorhombic
Space group	Fdd2
<i>a</i> [\AA]	22.1474(16)
<i>b</i> [\AA]	31.680(2)
<i>c</i> [\AA]	4.1140(3)
$\alpha$ [°]	90
$\beta$ [°]	90
$\gamma$ [°]	90
<i>V</i> [\AA <sup>3</sup> ]	2886.5(4)
<i>Z</i>	8
<i>T</i> [K]	150(2)
$\rho_{\text{calcd}}$ [Mg m <sup>-3</sup> ]	1.612
$\mu$ [mm <sup>-1</sup> ]	0.123
<i>F</i> (000)	1456
$\theta$ [°]	3.680 to 29.987°.
Index ranges	-30<=h<=30, -42<=k<=42, -5<=l<=5
Reflections collected	8232
Independent reflections ( <i>R</i> int)	2035 [ $R_{\text{int}} = 0.0474$ ]
Data/restraints/parameters	2035 / 3 / 114
GOF on <i>F</i> 2	1.022
<i>R</i> 1 ( <i>I</i> > 2δ( <i>I</i> )) <i>a</i>	0.0396
<i>wR</i> 2 ( <i>I</i> > 2δ( <i>I</i> )) <i>b</i>	0.0822
<i>R</i> 1 (all data)	0.0570
<i>wR</i> 2 (all data)	0.0883
Largest diff. peak and hole [e.Å <sup>-3</sup> ]	0.190 and -0.235
<hr/>	
<sub>a</sub> $R_1 = \sum  F_0  -  F_c  / \sum  F_0 $	<sub>b</sub> $R_2 = [\sum w(F_0^2 - F_c^2)^2 / \sum w(F_0^2)]^{1/2}$
<hr/>	

**Table S2.** Atomic coordinates (x 10<sup>4</sup>) and equivalent isotropic displacement parameters (Å<sup>2</sup> x 10<sup>3</sup>) for **4**. U(eq) is defined as one-third of the trace of the orthogonalized U<sup>ij</sup> tensor.

	x	y	z	U(eq)
N(1)	-544(1)	-532(1)	8082(4)	16(1)
N(2)	-1065(1)	-531(1)	9811(5)	18(1)
N(3)	-1331(1)	-162(1)	9501(5)	20(1)
N(4)	-989(1)	90(1)	7580(5)	19(1)
C(5)	-516(1)	-149(1)	6759(5)	14(1)

C(6)	0	0	4699(8)	17(1)
N(7)	0(1)	-2073(1)	208(6)	29(1)
C(8)	120(1)	-1708(1)	1743(6)	18(1)
N(9)	-258(1)	-1492(1)	3534(5)	21(1)
N(10)	91(1)	-1155(1)	4683(5)	20(1)
C(11)	649(1)	-1173(1)	3550(5)	17(1)
N(12)	1099(1)	-909(1)	4167(6)	25(1)
N(13)	678(1)	-1520(1)	1643(5)	16(1)

**Table S3.** Bond lengths [Å] and angles [°] for **4**.

N(1)-C(5)	1.331(3)	N(1)-N(2)	1.355(2)
N(2)-N(3)	1.317(2)	N(3)-N(4)	1.354(3)
N(4)-C(5)	1.335(3)	C(5)-C(6)	1.499(3)
C(6)-C(5)#1	1.499(3)	C(6)-H(6A)	0.9900
C(6)-H(6B)	0.9900	N(7)-C(8)	1.343(3)
N(7)-H(7A)	0.8800	N(7)-H(7B)	0.8800
C(8)-N(9)	1.307(3)	C(8)-N(13)	1.373(3)
N(9)-N(10)	1.401(3)	N(10)-C(11)	1.321(3)
N(10)-H(10)	0.8800	C(11)-N(12)	1.326(3)
C(11)-N(13)	1.352(3)	N(12)-H(12A)	0.8800
N(12)-H(12B)	0.8800	N(13)-H(13)	0.8800
C(5)-N(1)-N(2)	104.67(17)	N(3)-N(2)-N(1)	109.29(18)
N(2)-N(3)-N(4)	109.30(18)	C(5)-N(4)-N(3)	104.61(17)
N(1)-C(5)-N(4)	112.13(19)	N(1)-C(5)-C(6)	123.59(17)
N(4)-C(5)-C(6)	124.24(16)	C(5)#1-C(6)-C(5)	111.1(3)
C(5)#1-C(6)-H(6A)	109.4	C(5)-C(6)-H(6A)	109.4
C(5)#1-C(6)-H(6B)	109.4	C(5)-C(6)-H(6B)	109.4
H(6A)-C(6)-H(6B)	108.0	C(8)-N(7)-H(7A)	120.0
C(8)-N(7)-H(7B)	120.0	H(7A)-N(7)-H(7B)	120.0
N(9)-C(8)-N(7)	126.1(2)	N(9)-C(8)-N(13)	111.43(19)
N(7)-C(8)-N(13)	122.4(2)	C(8)-N(9)-N(10)	103.69(17)
C(11)-N(10)-N(9)	111.31(18)	C(11)-N(10)-H(10)	124.3
N(9)-N(10)-H(10)	124.3	N(10)-C(11)-N(12)	127.5(2)
N(10)-C(11)-N(13)	106.54(19)	N(12)-C(11)-N(13)	126.0(2)
C(11)-N(12)-H(12A)	120.0	C(11)-N(12)-H(12B)	120.0
H(12A)-N(12)-H(12B)	120.0	C(11)-N(13)-C(8)	107.00(18)
C(11)-N(13)-H(13)	126.5	C(8)-N(13)-H(13)	126.5

Symmetry transformations used to generate equivalent atoms:

#1 -x,-y,z

**Table S4.** Anisotropic displacement parameters ( $\text{\AA}^2 \times 10^3$ ) for DSR-BIS TM6. The anisotropic

displacement factor exponent takes the form:  $-2\pi^2[h^2a^*2U^{11} + \dots + 2hk a^* b^* U^{12}]$

U11	U22	U33	U23	U13	U12

N(1)	15(1)	15(1)	19(1)	-1(1)	3(1)	-1(1)
N(2)	15(1)	19(1)	21(1)	-1(1)	3(1)	0(1)
N(3)	17(1)	20(1)	24(1)	1(1)	2(1)	2(1)
N(4)	17(1)	18(1)	22(1)	2(1)	0(1)	2(1)
C(5)	15(1)	15(1)	14(1)	-1(1)	-2(1)	-2(1)
C(6)	18(2)	19(1)	15(1)	0	0	-3(1)
N(7)	20(1)	23(1)	43(1)	-12(1)	8(1)	-7(1)
C(8)	14(1)	16(1)	24(1)	2(1)	2(1)	0(1)
N(9)	16(1)	18(1)	30(1)	-4(1)	5(1)	-2(1)
N(10)	15(1)	17(1)	27(1)	-5(1)	7(1)	-1(1)
C(11)	15(1)	16(1)	19(1)	1(1)	3(1)	3(1)
N(12)	15(1)	21(1)	39(1)	-13(1)	7(1)	-2(1)
N(13)	13(1)	15(1)	21(1)	-3(1)	6(1)	0(1)

**Table S5.** Hydrogen coordinates ( $\times 10^4$ ) and isotropic displacement parameters ( $\text{\AA}^2 \times 10^3$ ) for 4.

	x	y	z	U(eq)
H(6A)	138	-234	3285	20
H(6B)	-138	234	3285	20
H(7A)	-360	-2188	363	34
H(7B)	283	-2197	-953	34
H(10)	-44	-956	5993	24
H(12A)	1042	-692	5467	30
H(12B)	1455	-951	3275	30
H(13)	994	-1608	545	20

**Table S6.** Torsion angles [°] for 4.

C(5)-N(1)-N(2)-N(3)	0.1(2)
N(1)-N(2)-N(3)-N(4)	-0.4(2)
N(2)-N(3)-N(4)-C(5)	0.6(2)
N(2)-N(1)-C(5)-N(4)	0.3(2)
N(2)-N(1)-C(5)-C(6)	178.0(2)
N(3)-N(4)-C(5)-N(1)	-0.5(3)
N(3)-N(4)-C(5)-C(6)	-178.2(2)
N(1)-C(5)-C(6)-C(5)#1	-82.0(2)
N(4)-C(5)-C(6)-C(5)#1	95.5(2)
N(7)-C(8)-N(9)-N(10)	177.2(2)
N(13)-C(8)-N(9)-N(10)	-1.5(3)
C(8)-N(9)-N(10)-C(11)	0.9(3)
N(9)-N(10)-C(11)-N(12)	-179.1(2)
N(9)-N(10)-C(11)-N(13)	0.0(3)
N(10)-C(11)-N(13)-C(8)	-0.9(2)
N(12)-C(11)-N(13)-C(8)	178.3(2)
N(9)-C(8)-N(13)-C(11)	1.6(3)
N(7)-C(8)-N(13)-C(11)	-177.1(2)

Symmetry transformations used to generate equivalent atoms:  
#1 -x,-y,z

**Table S7.** Hydrogen bonds for 4 [Å and °].

D-H...A	d(D-H)	d(H...A)	d(D...A)	<(DHA)
N(7)-H(7B)...N(3)#3	0.88	2.18	3.025(3)	160.2
N(10)-H(10)...N(1)	0.88	1.94	2.799(3)	163.5
N(12)-H(12A)...N(4)#1	0.88	2.10	2.960(3)	165.7
N(12)-H(12B)...N(9)#4	0.88	1.98	2.858(3)	175.5
N(13)-H(13)...N(2)#3	0.88	2.01	2.831(3)	155.4

Symmetry transformations used to generate equivalent atoms:  
#1 -x,-y,z #2 -x-1/4,y-1/4,z-3/4 #3 x+1/4,-y-1/4,z-5/4  
#4 x+1/4,-y-1/4,z-1/4

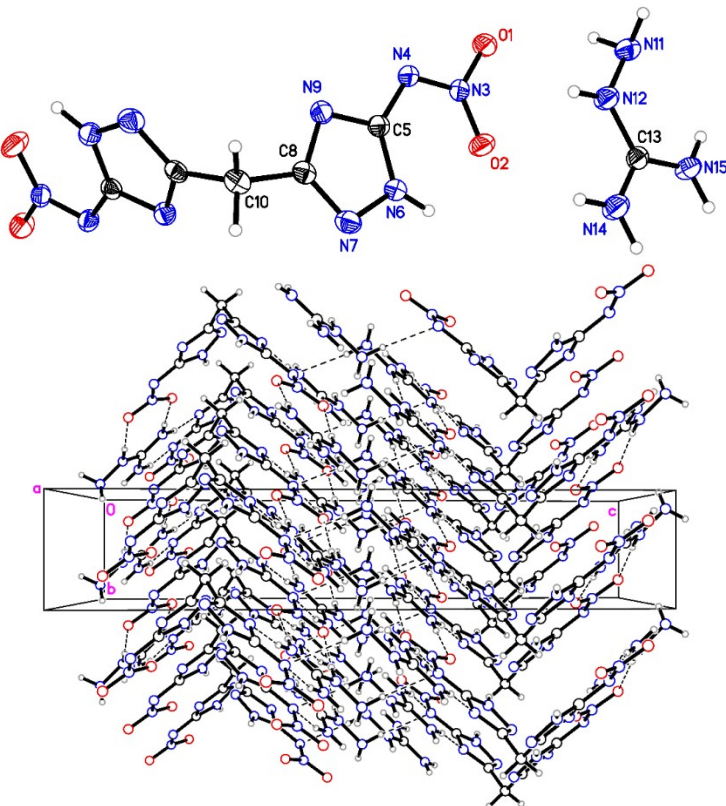


**Figure S2.** Molecular structure and crystal packing of **15**.

**Table S8:** Crystallographic data for **15**.

Compound	15
Formula	C <sub>7</sub> H <sub>18</sub> N <sub>18</sub> O <sub>4</sub>
CCDC number	2113930
Mw	418.39
Crystal size [mm3]	0.600 x 0.051 x 0.020
Crystal system	Monoclinic
Space group	C2/c
<i>a</i> [Å]	16.231(5)
<i>b</i> [Å]	4.4470(9)
<i>c</i> [Å]	23.508(7)
$\alpha$ [°]	90
$\beta$ [°]	94.7
$\gamma$ [°]	90
<i>V</i> [Å <sup>3</sup> ]	1691.0(8)
Z	4
<i>T</i> [K]	150(2)
$\rho_{\text{calcd}}$ [Mg m <sup>-3</sup> ]	1.643
$\mu$ [mm <sup>-1</sup> ]	1.176
<i>F</i> (000)	872
$\theta$ [°]	3.773 to 68.244
Index ranges	-16<=h<=19, -4<=k<=5, -26<=l<=27
Reflections collected	4433
Independent reflections ( <i>R</i> int)	1454 [ $R_{\text{int}} = 0.0581$ ]
Data/restraints/parameters	1454 / 3 / 147
GOF on <i>F</i> 2	1.081
<i>R</i> 1 ( <i>I</i> > 2δ( <i>I</i> )) <i>a</i>	0.0449
<i>wR</i> 2 ( <i>I</i> > 2δ( <i>I</i> )) <i>b</i>	0.1071
<i>R</i> 1 (all data)	0.0571
<i>wR</i> 2 (all data)	0.1165
Largest diff. peak and hole [e.Å <sup>-3</sup> ]	0.245 and -0.271

---


$${}_a R_1 = \sum ||F_0| - |F_c|| / \sum |F_0| \quad {}_b R_2 = [\sum w(F_0^2 - F_c^2)^2 / \sum w(F_0^2)^2]^{1/2}$$


---

**Table S9:** Atomic coordinates ( $x \times 10^4$ ) and equivalent isotropic displacement parameters ( $\text{\AA}^2 \times 10^3$ ) for 15.  $U(\text{eq})$  is defined as one-third of the trace of the orthogonalized  $U_{ij}$  tensor.

	x	y	z	$U(\text{eq})$
O(1)	2285(1)	7300(4)	4311(1)	31(1)
O(2)	2757(1)	5267(4)	3551(1)	36(1)
N(3)	2186(1)	5627(4)	3872(1)	23(1)
N(4)	1469(1)	4311(4)	3786(1)	23(1)
C(5)	1352(1)	2384(5)	3325(1)	20(1)
N(6)	1863(1)	1380(4)	2943(1)	23(1)
N(7)	1449(1)	-627(4)	2578(1)	26(1)
C(8)	702(1)	-674(5)	2763(1)	20(1)
N(9)	610(1)	1119(4)	3221(1)	21(1)
C(10)	0	-2556(7)	2500	23(1)
N(11)	3801(1)	3521(4)	4961(1)	26(1)
N(12)	3709(1)	1293(5)	4535(1)	26(1)
C(13)	4351(1)	568(5)	4240(1)	22(1)
N(14)	4247(1)	-1494(5)	3835(1)	29(1)
N(15)	5074(1)	1892(4)	4356(1)26(1)	

---

**Table S10.** Bond lengths [ $\text{\AA}$ ] and angles [ $^\circ$ ] for 15.

O(1)-N(3)	1.272(2)	O(2)-N(3)	1.251(2)
N(3)-N(4)	1.304(3)	N(4)-C(5)	1.382(3)
C(5)-N(9)	1.334(3)	C(5)-N(6)	1.347(3)
N(6)-N(7)	1.375(3)	N(6)-H(6)	0.88(3)
N(7)-C(8)	1.322(3)	C(8)-N(9)	1.358(3)
C(8)-C(10)	1.506(3)	C(10)-C(8)#1	1.506(3)
C(10)-H(10A)	0.9900	C(10)-H(10B)	0.9900
N(11)-N(12)	1.408(3)	N(11)-H(11A)	0.907(10)
N(11)-H(11B)	0.910(10)	N(12)-C(13)	1.337(3)
N(12)-H(12)	0.89(3)	C(13)-N(15)	1.322(3)
C(13)-N(14)	1.323(3)	N(14)-H(14A)	0.8800
N(14)-H(14B)	0.8800	N(15)-H(15A)	0.8800
N(15)-H(15B)	0.8800		
O(2)-N(3)-O(1)	120.89(19)	O(2)-N(3)-N(4)	123.01(18)
O(1)-N(3)-N(4)	116.09(18)	N(3)-N(4)-C(5)	117.56(18)
N(9)-C(5)-N(6)	109.55(19)	N(9)-C(5)-N(4)	117.88(19)

N(6)-C(5)-N(4)	132.5(2)	C(5)-N(6)-N(7)	109.63(19)
C(5)-N(6)-H(6)	127.4(18)	N(7)-N(6)-H(6)	122.9(18)
C(8)-N(7)-N(6)	102.60(18)	N(7)-C(8)-N(9)	114.6(2)
N(7)-C(8)-C(10)	123.84(18)	N(9)-C(8)-C(10)	121.56(18)
C(5)-N(9)-C(8)	103.62(19)	C(8)-C(10)-C(8)#1	112.4(3)
C(8)-C(10)-H(10A)	109.1	C(8)#1-C(10)-H(10A)	109.1
C(8)-C(10)-H(10B)	109.1	C(8)#1-C(10)-H(10B)	109.1
H(10A)-C(10)-H(10B)	107.9	N(12)-N(11)-H(11A)	110.3(16)
N(12)-N(11)-H(11B)	107.9(17)	H(11A)-N(11)-H(11B)	109.0(17)
C(13)-N(12)-N(11)	119.8(2)	C(13)-N(12)-H(12)	116.0(19)
N(11)-N(12)-H(12)	124.0(19)	N(15)-C(13)-N(14)	121.0(2)
N(15)-C(13)-N(12)	120.1(2)	N(14)-C(13)-N(12)	118.8(2)
C(13)-N(14)-H(14A)	120.0	C(13)-N(14)-H(14B)	120.0
H(14A)-N(14)-H(14B)	120.0	C(13)-N(15)-H(15A)	120.0
C(13)-N(15)-H(15B)	120.0	H(15A)-N(15)-H(15B)	120.0

Symmetry transformations used to generate equivalent atoms:

#1 -x,y,-z+1/2

**Table S11.** Anisotropic displacement parameters ( $\text{\AA}^2 \times 10^3$ ) for 15. The anisotropic displacement factor exponent takes the form:  $-2\pi^2[h^2a^*a^*U_{11} + \dots + 2hka^*b^*U_{12}]$

	U11	U22	U33	U23	U13	U12
O(1)	26(1)	41(1)	27(1)	-14(1)	2(1)	-3(1)
O(2)	22(1)	54(1)	33(1)	-14(1)	9(1)	-7(1)
N(3)	19(1)	28(1)	22(1)	-2(1)	0(1)	3(1)
N(4)	19(1)	28(1)	21(1)	-4(1)	2(1)	-1(1)
C(5)	22(1)	20(1)	18(1)	3(1)	1(1)	5(1)
N(6)	21(1)	27(1)	20(1)	-3(1)	2(1)	1(1)
N(7)	29(1)	28(1)	21(1)	-3(1)	3(1)	1(1)
C(8)	24(1)	17(1)	17(1)	4(1)	0(1)	4(1)
N(9)	21(1)	22(1)	21(1)	-1(1)	1(1)	1(1)
C(10)	30(2)	20(2)	21(2)	0	1(1)	0
N(11)	26(1)	26(1)	25(1)	-2(1)	7(1)	3(1)
N(12)	21(1)	30(1)	27(1)	-5(1)	5(1)	-2(1)
C(13)	21(1)	22(1)	21(1)	5(1)	3(1)	3(1)
N(14)	21(1)	34(1)	33(1)	-8(1)	6(1)	-1(1)
N(15)	23(1)	28(1)	29(1)	-4(1)	8(1)	1(1)

**Table S12.** Hydrogen coordinates ( $x \times 10^4$ ) and isotropic displacement parameters ( $\text{\AA}^2 \times 10^3$ ) for 15.

	x	y	z	U(eq)
H(6)	2376(19)	1950(60)	2907(11)	32(7)
H(10A)	-208	-3867	2797	28
H(10B)	208	-3867	2203	28

H(11A)	3424(13)	5010(40)	4888(10)	31
H(11B)	3713(15)	2650(50)	5301(7)	31
H(12)	3250(20)	200(70)	4461(12)	42(8)
H(14A)	4663	-2003	3637	35
H(14B)	3762	-2355	3762	35
H(15A)	5497	1406	4162	32
H(15B)	5134	3260	4627	32

**Table S13.** Torsion angles [°] for 15.

O(2)-N(3)-N(4)-C(5)	1.6(3)
O(1)-N(3)-N(4)-C(5)	-177.55(19)
N(3)-N(4)-C(5)-N(9)	-177.50(19)
N(3)-N(4)-C(5)-N(6)	4.7(4)
N(9)-C(5)-N(6)-N(7)	-0.4(2)
N(4)-C(5)-N(6)-N(7)	177.5(2)
C(5)-N(6)-N(7)-C(8)	0.7(2)
N(6)-N(7)-C(8)-N(9)	-0.7(2)
N(6)-N(7)-C(8)-C(10)	179.80(19)
N(6)-C(5)-N(9)-C(8)	0.0(2)
N(4)-C(5)-N(9)-C(8)	-178.23(18)
N(7)-C(8)-N(9)-C(5)	0.4(3)
C(10)-C(8)-N(9)-C(5)	179.96(19)
N(7)-C(8)-C(10)-C(8)#1	-115.2(2)
N(9)-C(8)-C(10)-C(8)#1	65.29(18)
N(11)-N(12)-C(13)-N(15)	1.4(3)
N(11)-N(12)-C(13)-N(14)	-178.8(2)

Symmetry transformations used to generate equivalent atoms:

#1 -x,y,-z+1/2

**Table S14.** Hydrogen bonds for 15 [Å and °].

D-H...A	d(D-H)	d(H...A)	d(D...A)	<(DHA)
N(11)-H(11B)...N(4)#4	0.910(10)	2.358(10)	3.267(3)	176(2)
N(12)-H(12)...O(1)#5	0.89(3)	2.04(3)	2.929(3)	174(3)
N(14)-H(14A)...N(9)#6	0.88	2.06	2.936(3)	170.9
N(14)-H(14B)...O(2)#5	0.88	1.97	2.847(3)	172.1
N(15)-H(15A)...N(4)#6	0.88	2.09	2.955(3)	167.2
N(15)-H(15B)...N(11)#7	0.88	2.39	3.097(3)	137.8

Symmetry transformations used to generate equivalent atoms:

#1 -x,y,-z+1/2 #2 -x+1/2,y+1/2,-z+1/2 #3 -x+1/2,-y+3/2,-z+1

#4 -x+1/2,-y+1/2,-z+1 #5 x,y-1,z #6 x+1/2,y-1/2,z

#7 -x+1,-y+1,-z+1

**Table S15.** Nitrogen, oxygen content, volume of gaseous detonation products and detonation temperatures of compounds **3** to **16** compared with RDX, TATB and TNT.

Salt	N <sup>a</sup> %	O <sup>b</sup> %	V <sup>c</sup> (cm <sup>3</sup> /g)	D <sub>T</sub> <sup>d</sup> (K)
<b>3</b>	73.65	0	0.5	2460
<b>4</b>	71.97	0	0.5	2208
<b>5</b>	78.24	0	0.48	2908
<b>6</b>	79.52	0	0.48	2931
<b>7</b>	69.28	0	0.46	1860
<b>10</b>	55.25	21.04	0.44	2882
<b>11</b>	58.67	19.15	0.47	2910
<b>12</b>	49.99	28.55	0.46	3299
<b>13</b>	59.81	13.66	0.45	2562
<b>14</b>	57.52	14.60	0.46	2917
<b>15</b>	60.27	15.30	0.49	2462
<b>16</b>	62.96	11.06	0.45	2755
<b>RDX</b>	37.84	43.22	0.42	3734
<b>TNT</b>	18.50	42.26	0.46	3170
<b>TATB</b>	32.56	37.19	0.40	2749

<sup>a</sup>Nitrogen content; <sup>b</sup>Oxygen content; <sup>c</sup>Volume of gaseous detonation products; <sup>d</sup>Detonation temperature.

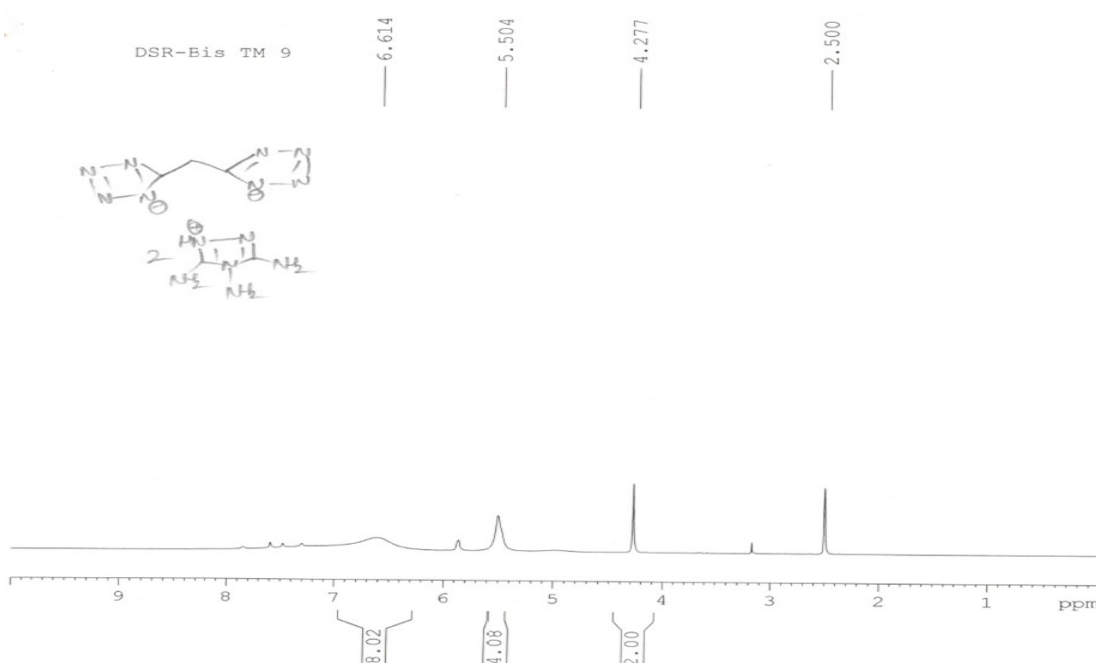


**Figure S4:**  $^1\text{H}$  NMR spectrum of **3**.

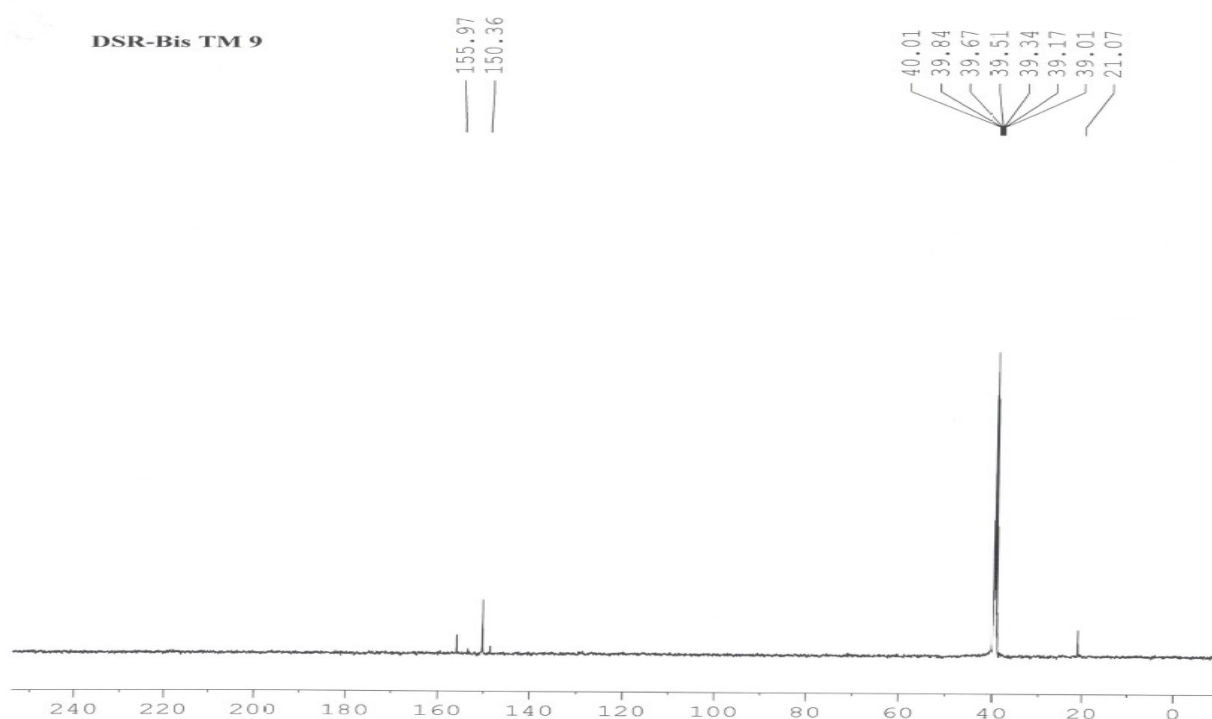


**Figure S5:**  $^{13}\text{C}$  NMR spectrum of **3**.

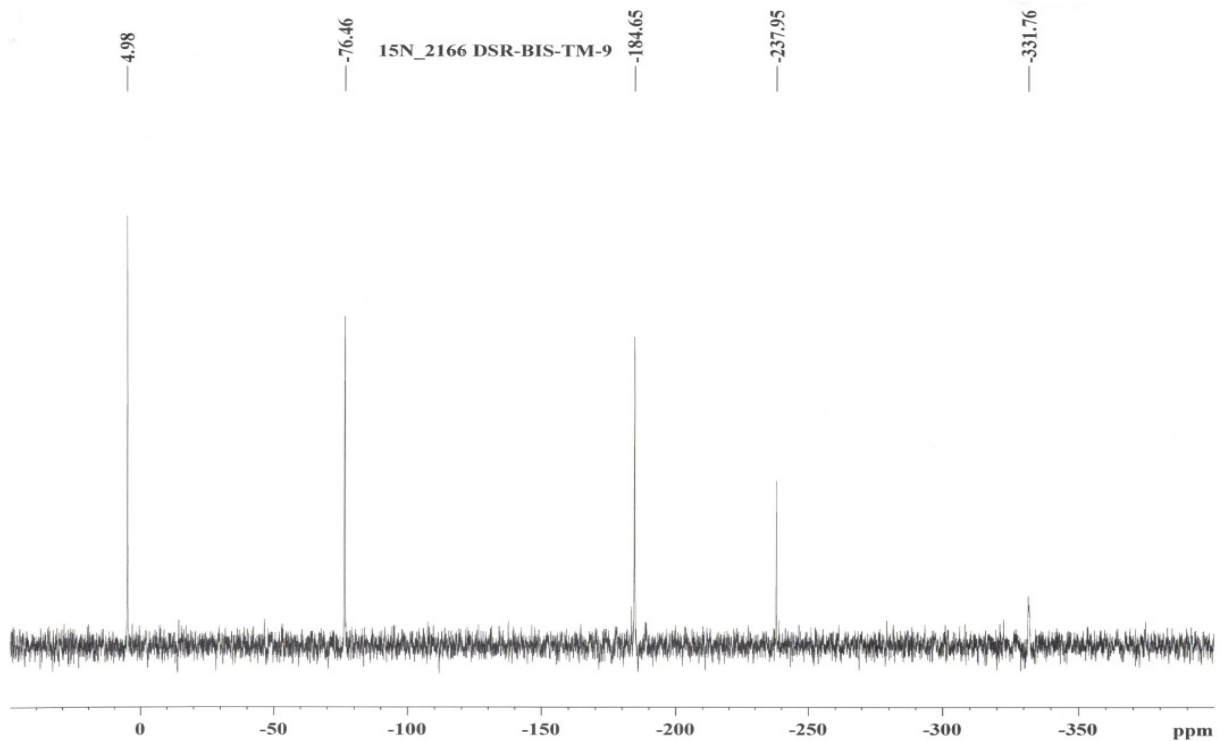


**Figure S6:**  $^{15}\text{N}$  NMR spectrum of **3**.

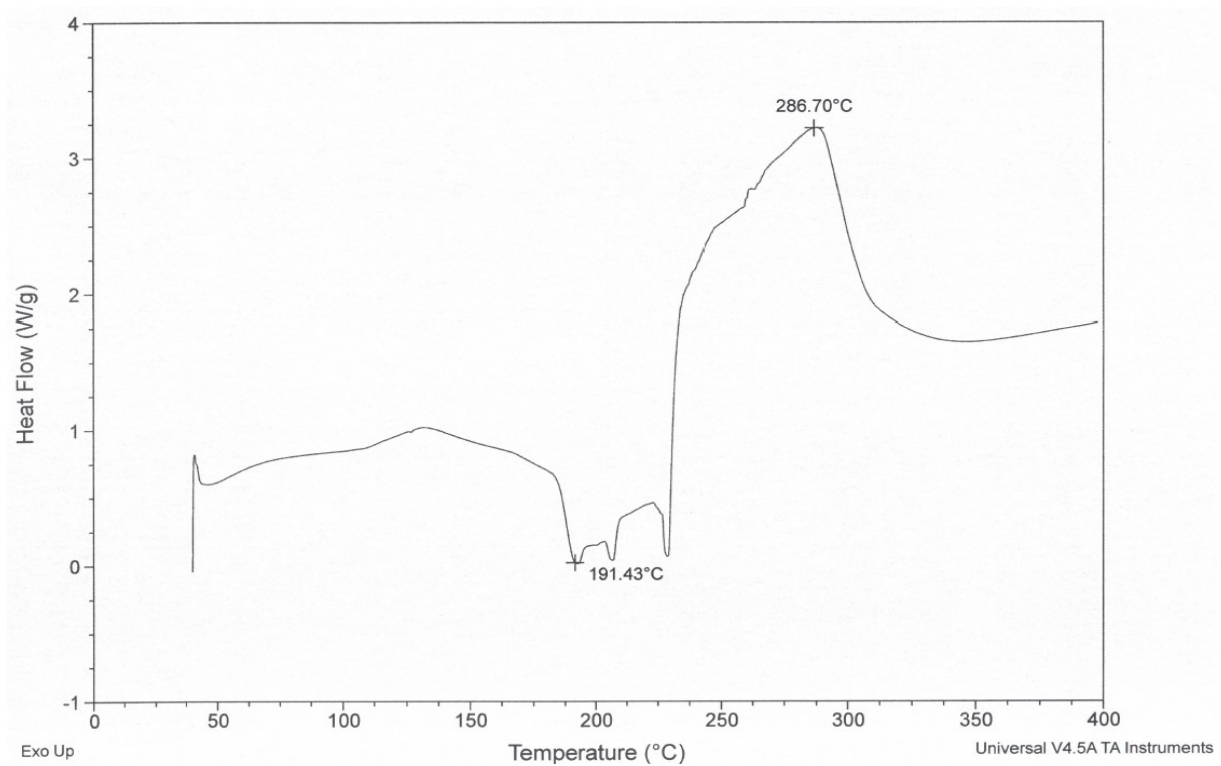


**Figure S7:** DSC plot of **3**.

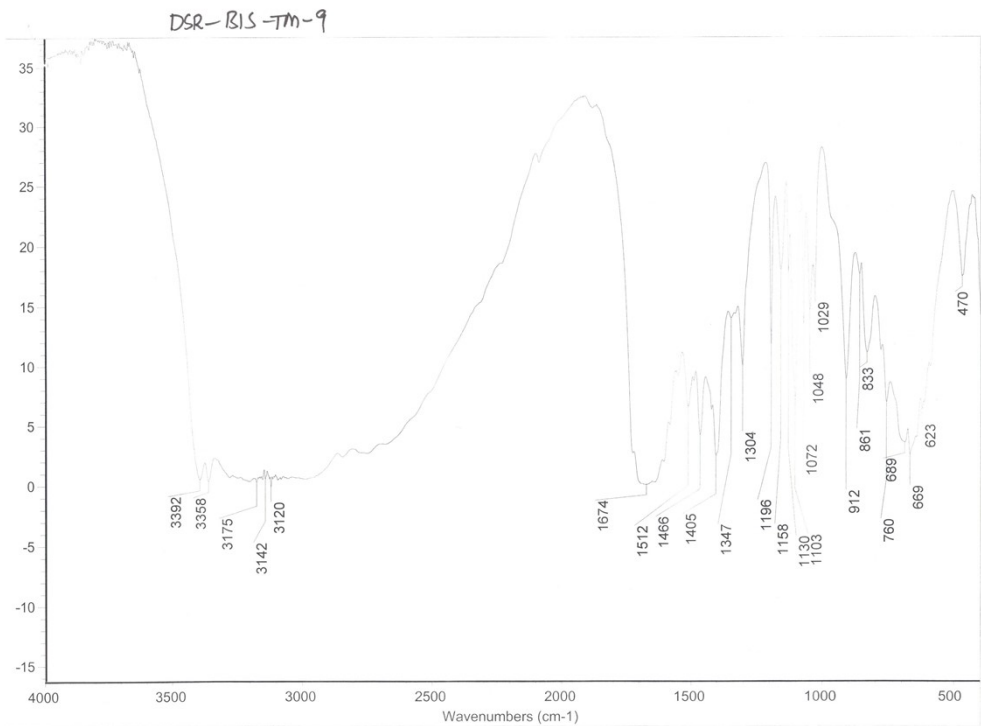


**Figure S8:** IR Spectrum of 3.

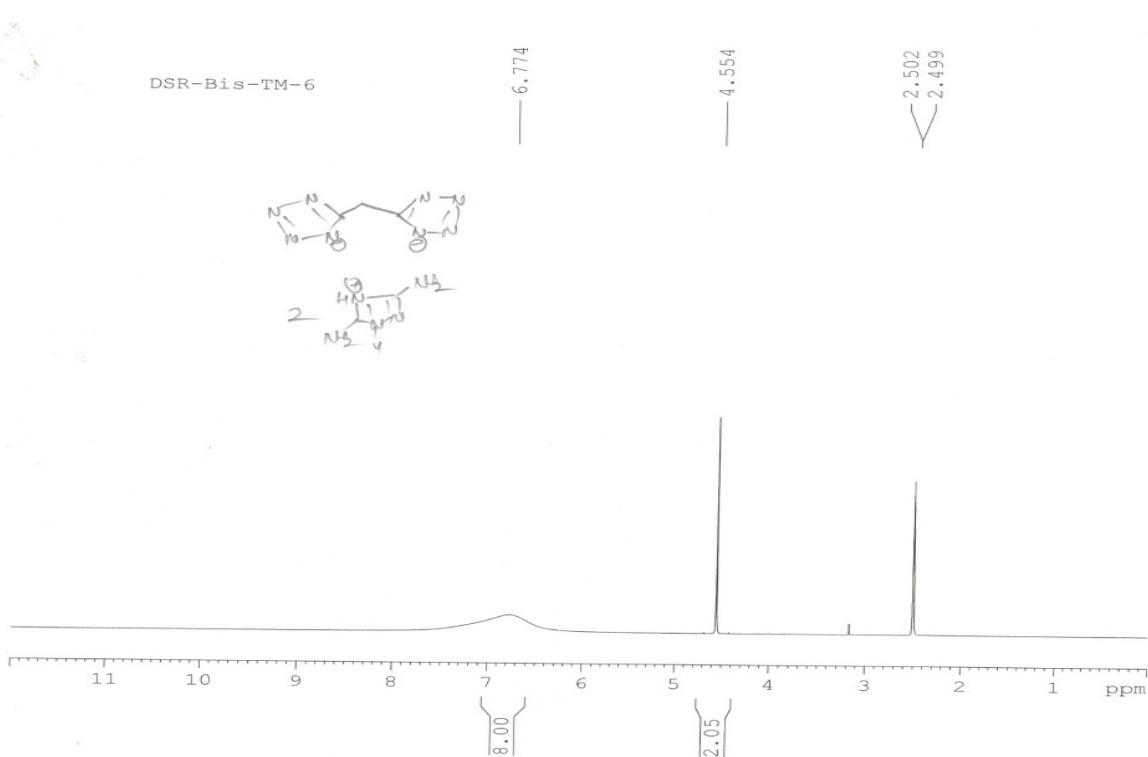


**Figure S9:**  $^1\text{H}$  NMR spectrum of **4**.

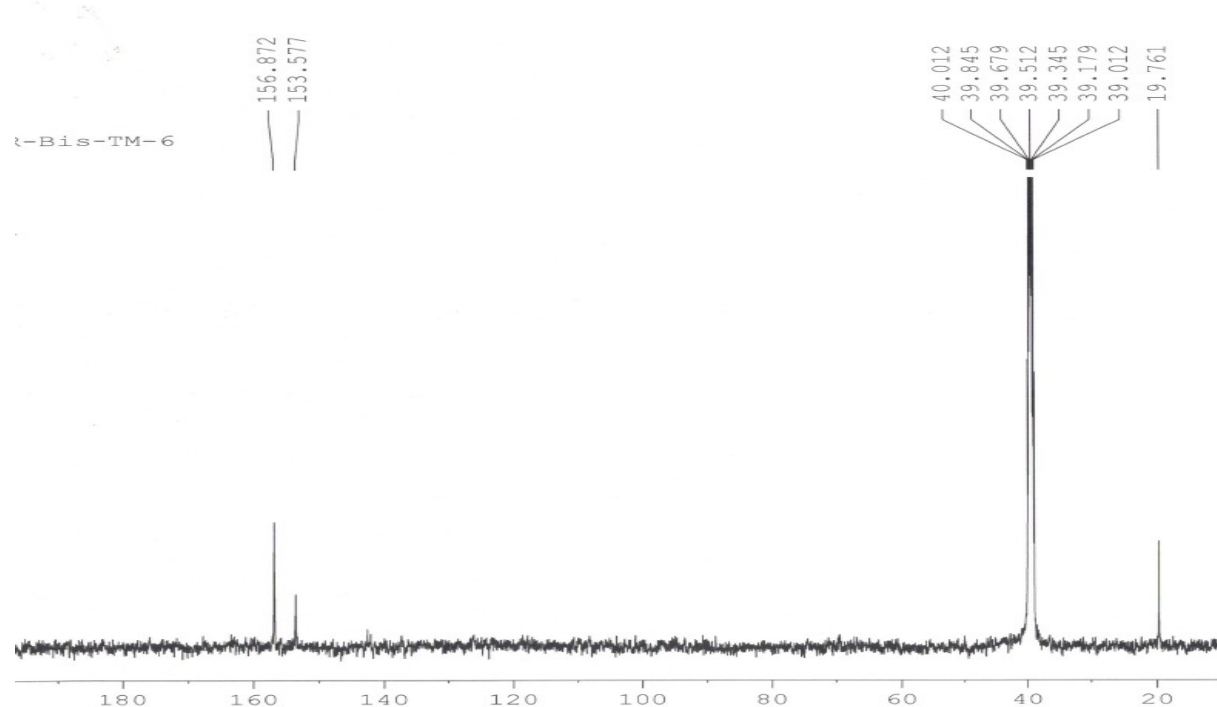


**Figure S10:**  $^{13}\text{C}$  NMR spectrum of **4**.

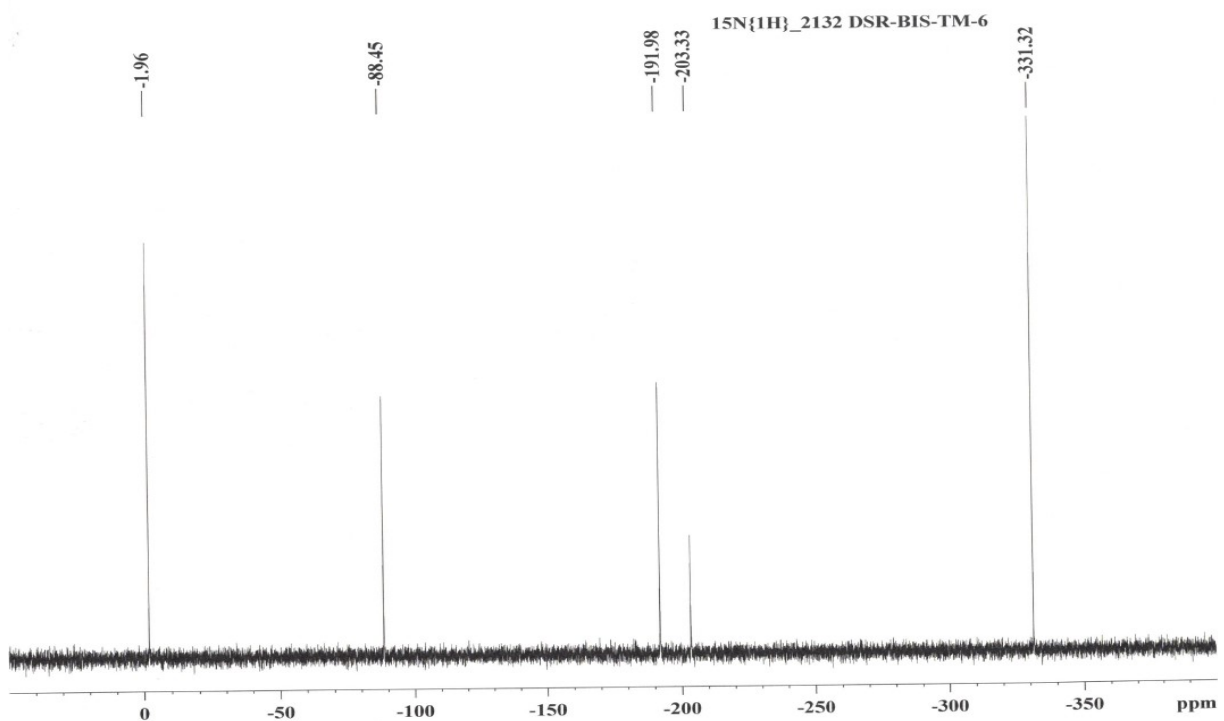


**Figure S11:**  $^{15}\text{N}$  NMR spectrum of 4.

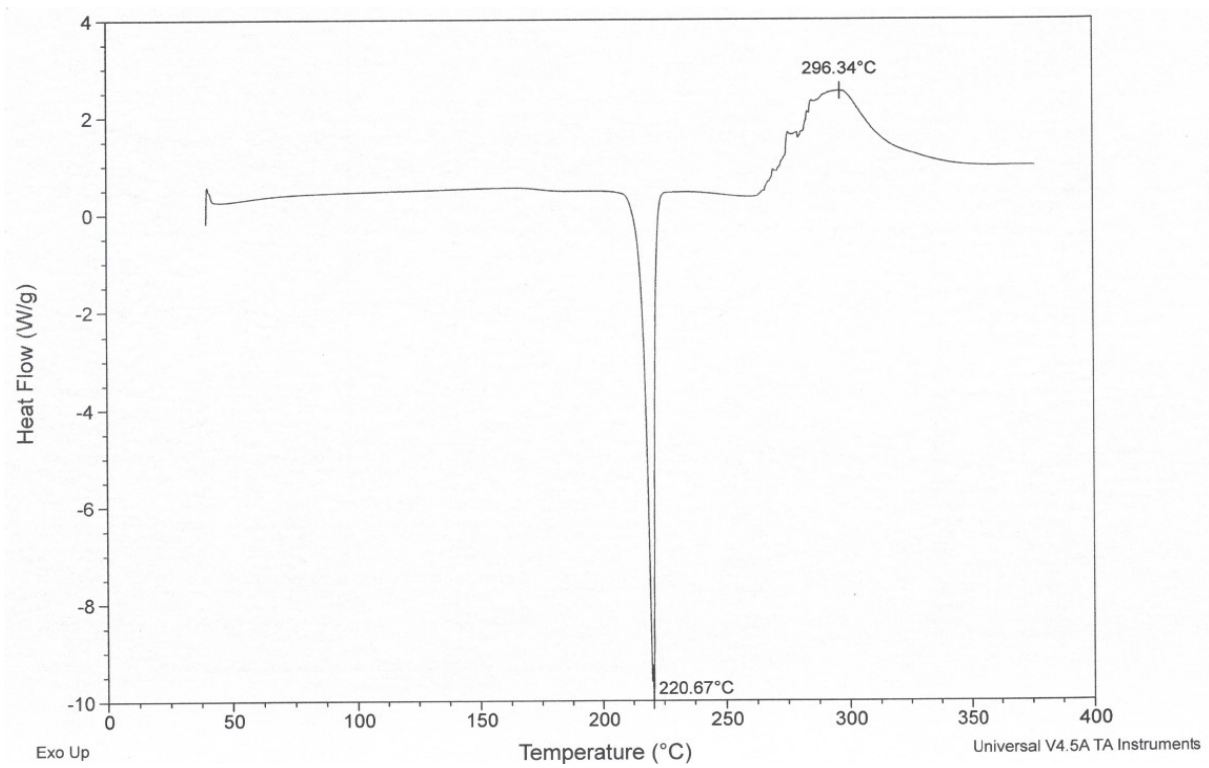


**Figure S12:** DSC plot of 4.

BIS-TM -6

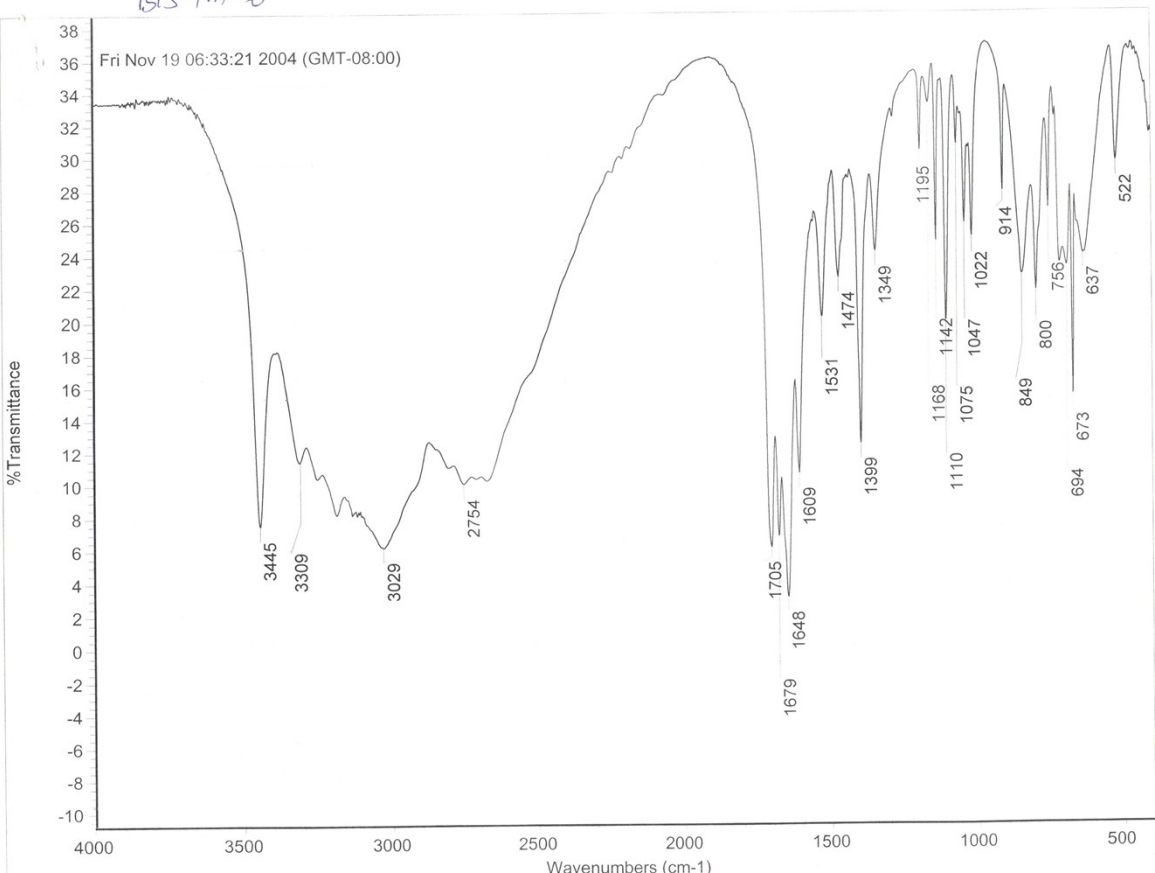


**Figure S13:** IR spectrum of **4**.

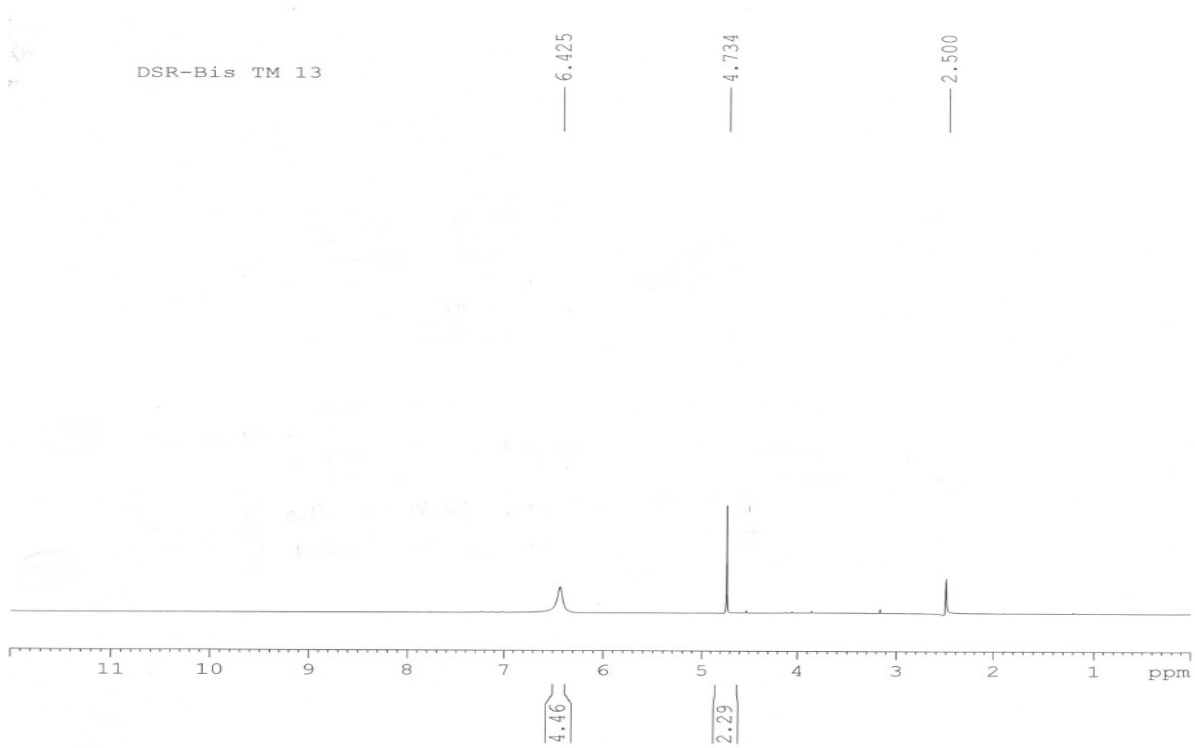


**Figure S14:**  $^1\text{H}$  NMR spectrum of **5**.

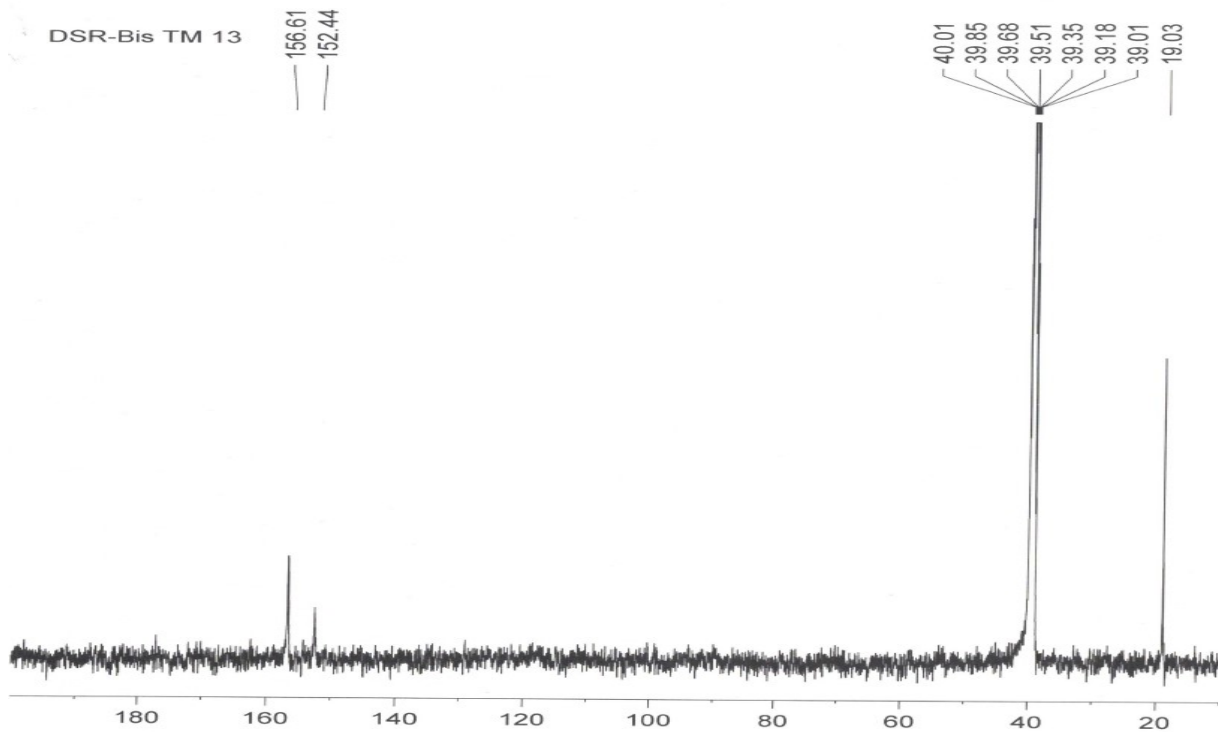


**Figure S15:**  $^{13}\text{C}$  NMR spectrum of **5**.

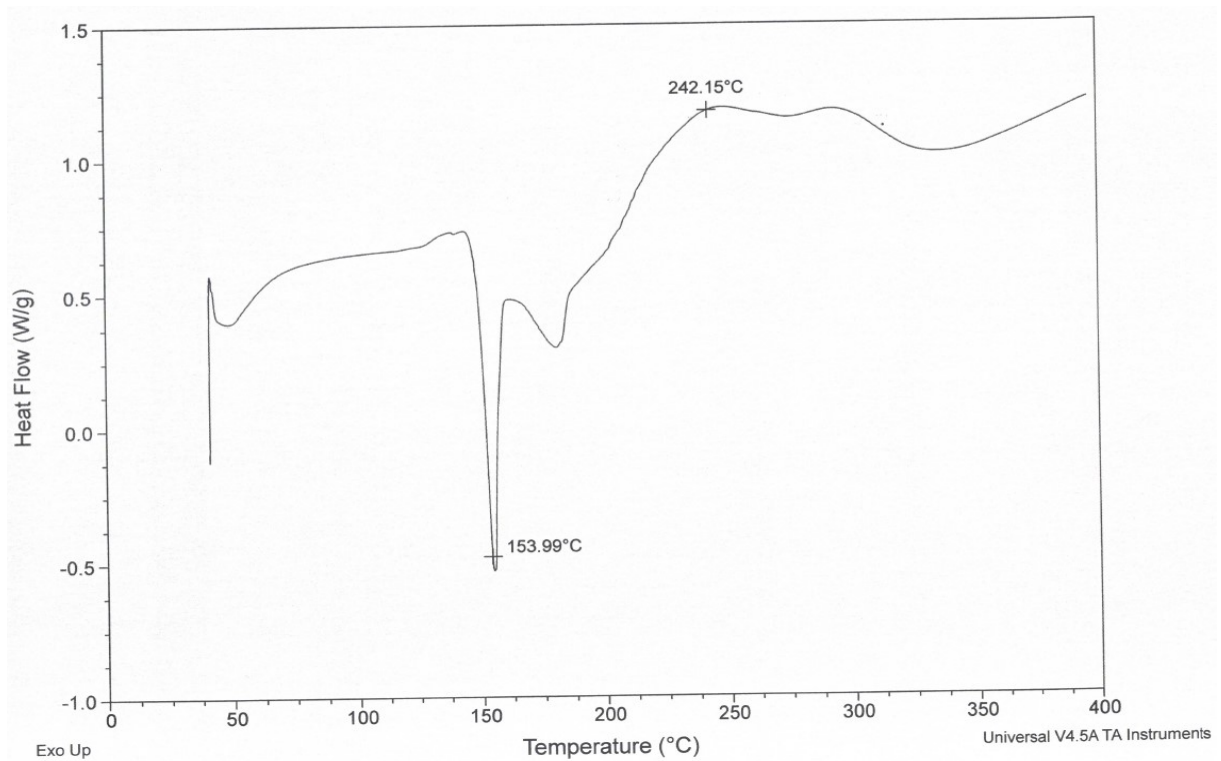


**Figure S16:** DSC plot of **5**.

DSR-BIS-TM-13

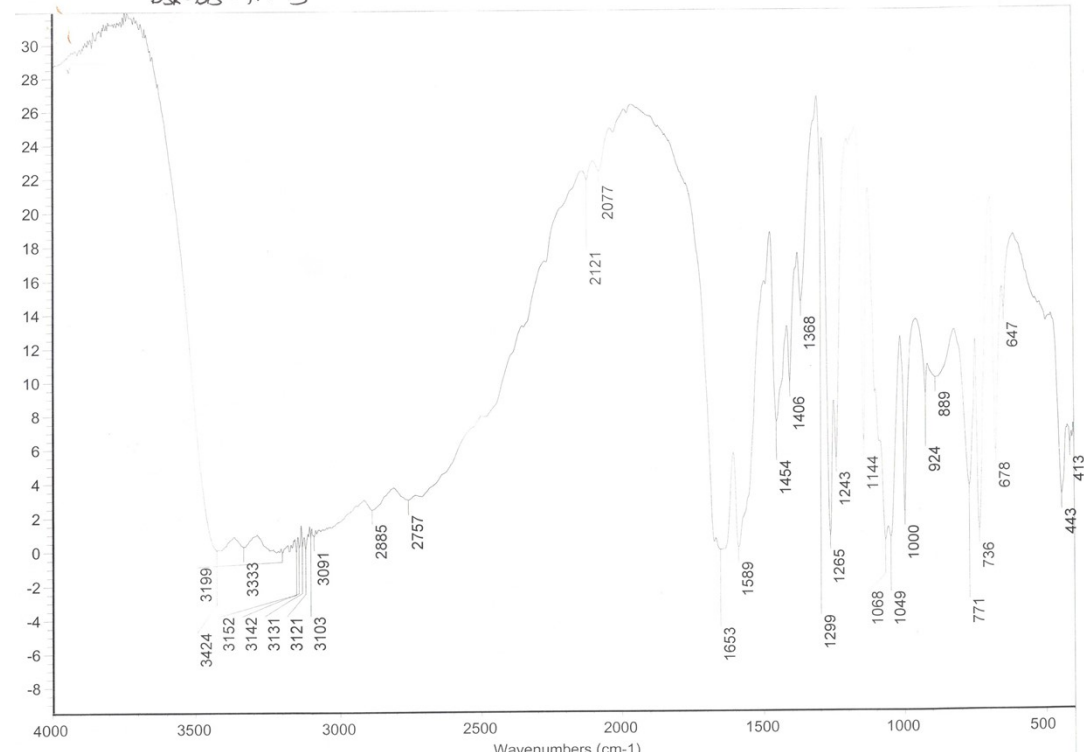
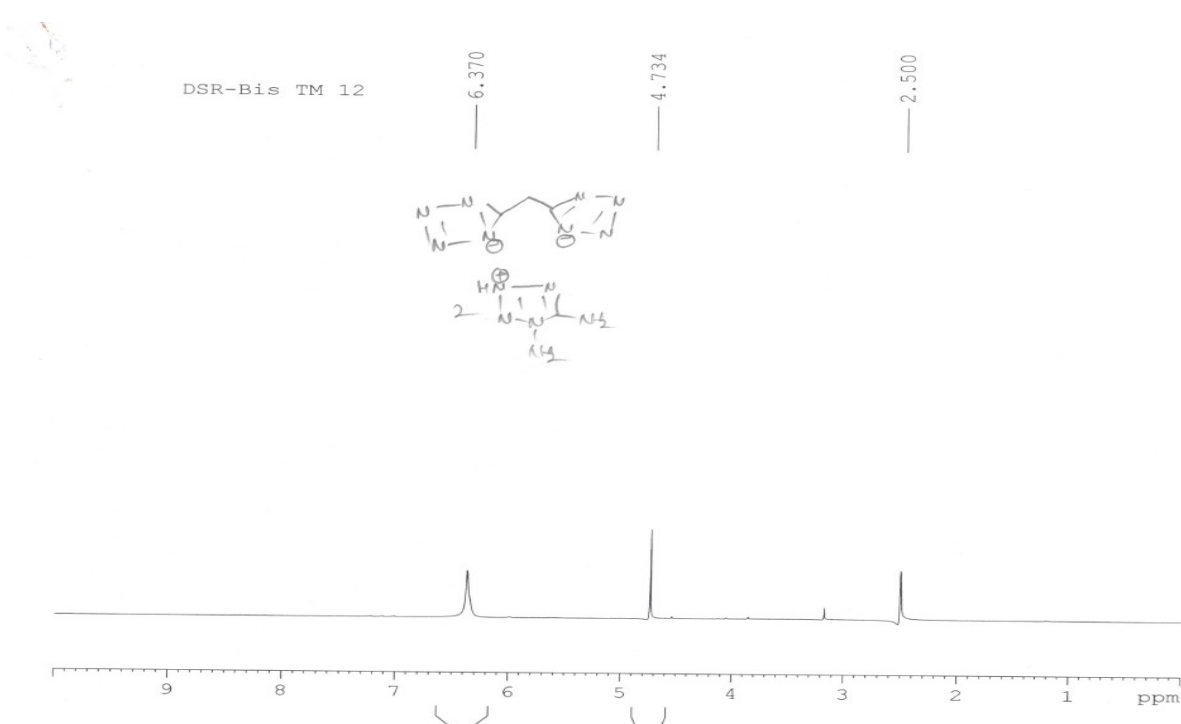
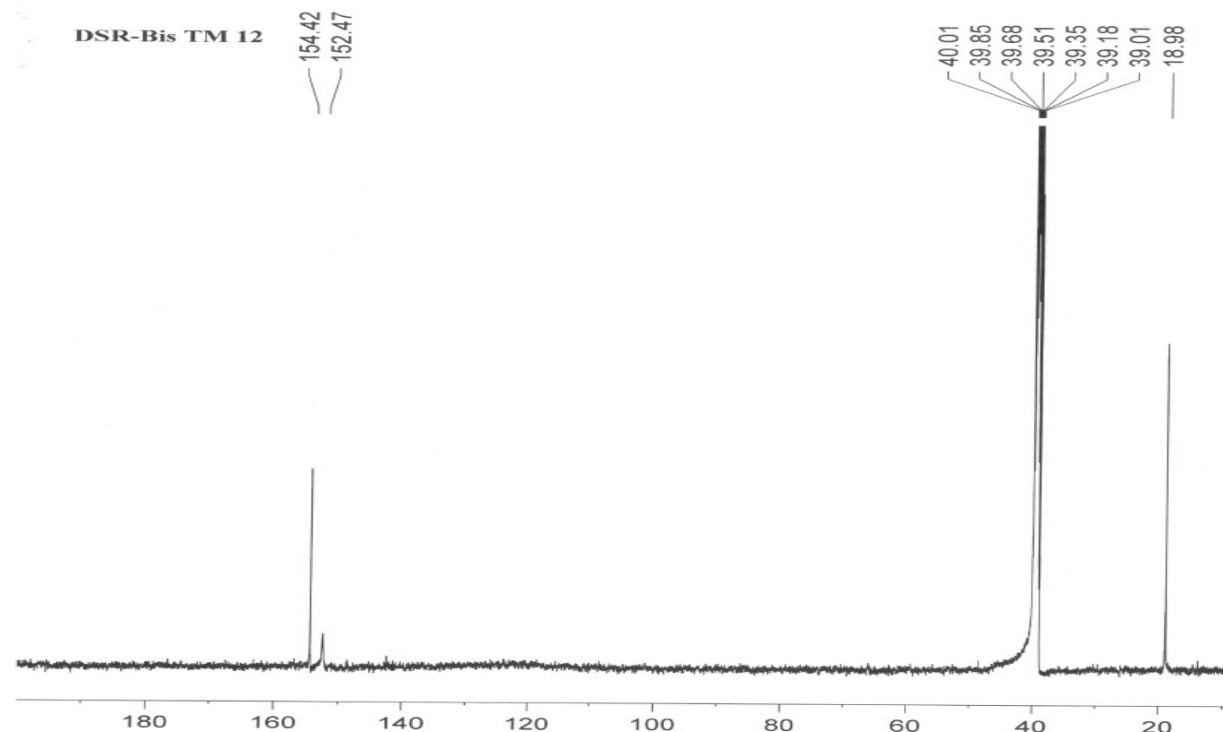


Figure S17: IR spectrum of 5.



**Figure S18:**  $^1\text{H}$  NMR spectrum of **6**.



**Figure S19:**  $^{13}\text{C}$  NMR spectrum of **6**.

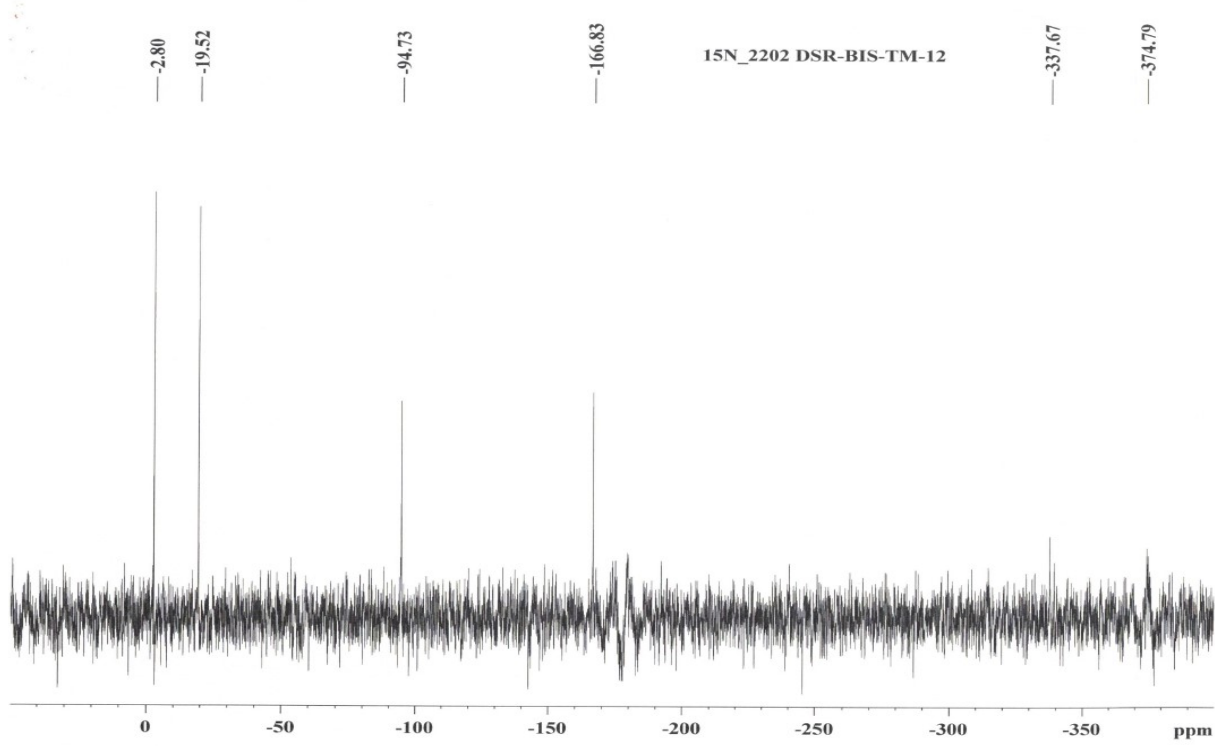


**Figure S20:** <sup>15</sup>N NMR spectrum of **6**.

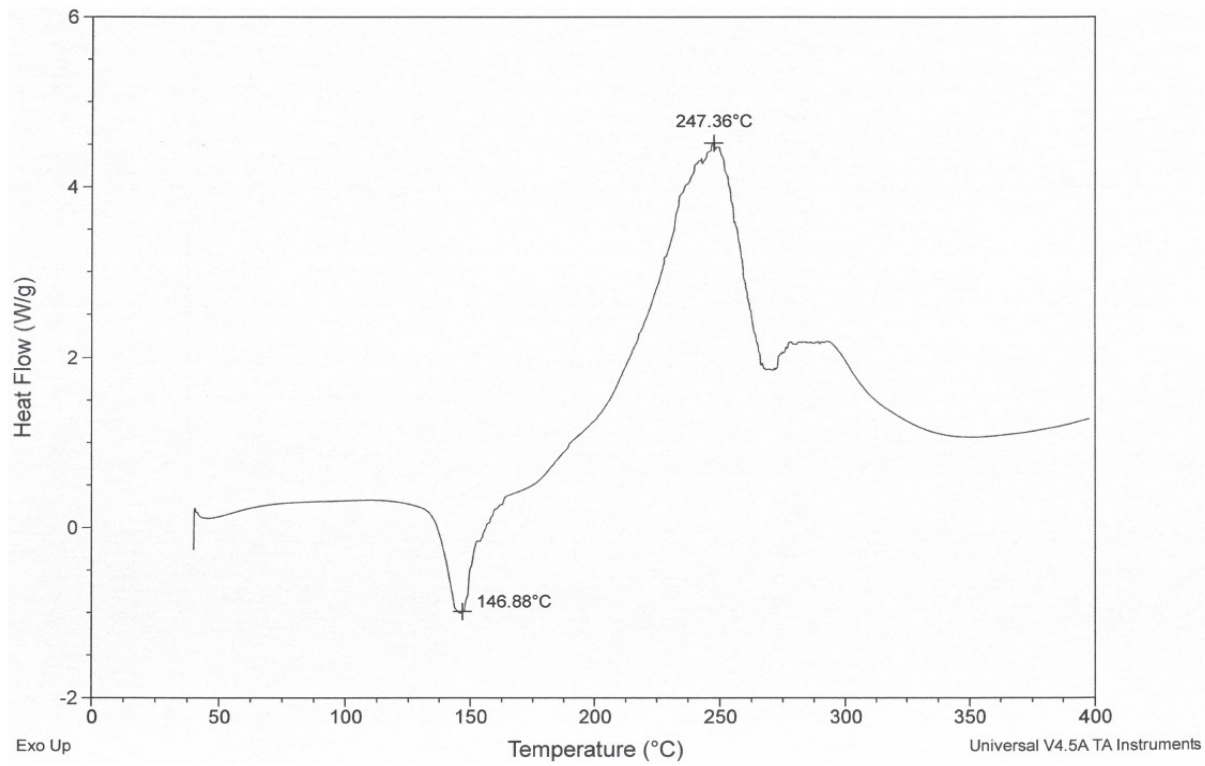


**Figure S21:** DSC plot of **6**.

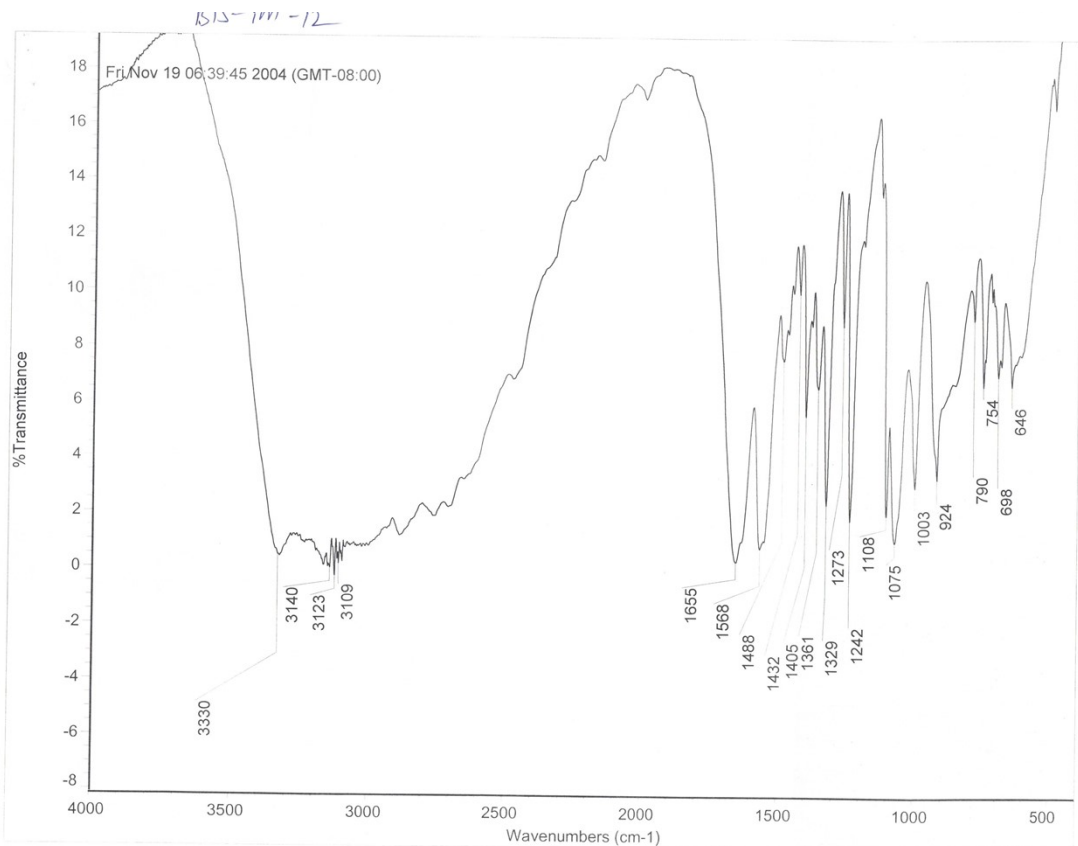


**Figure S22:** IR spectrum of **6**.

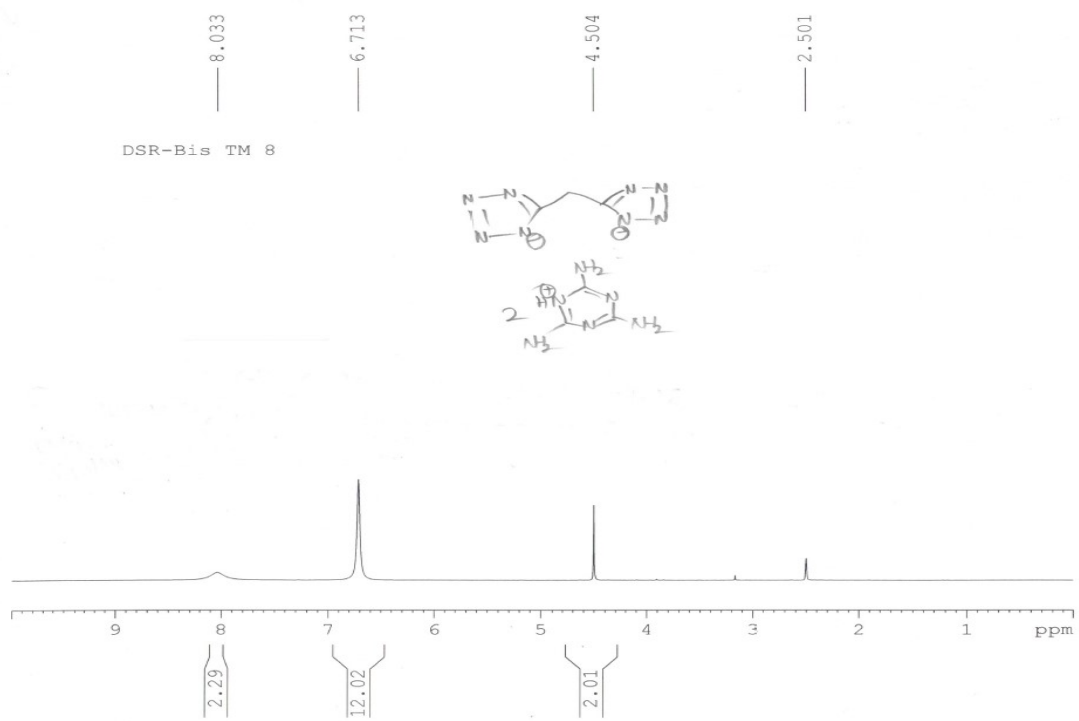


**Figure S23:**  $^1\text{H}$  NMR spectrum of 7.

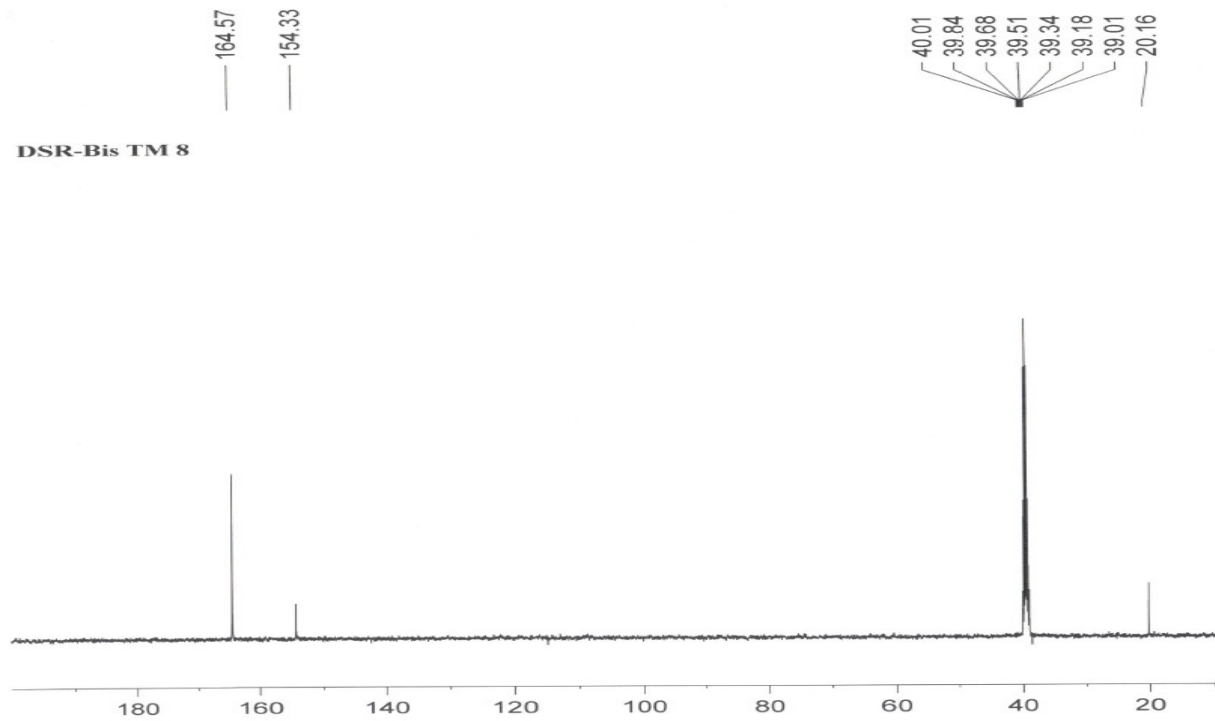


**Figure S24:**  $^{13}\text{C}$  NMR spectrum of 7.

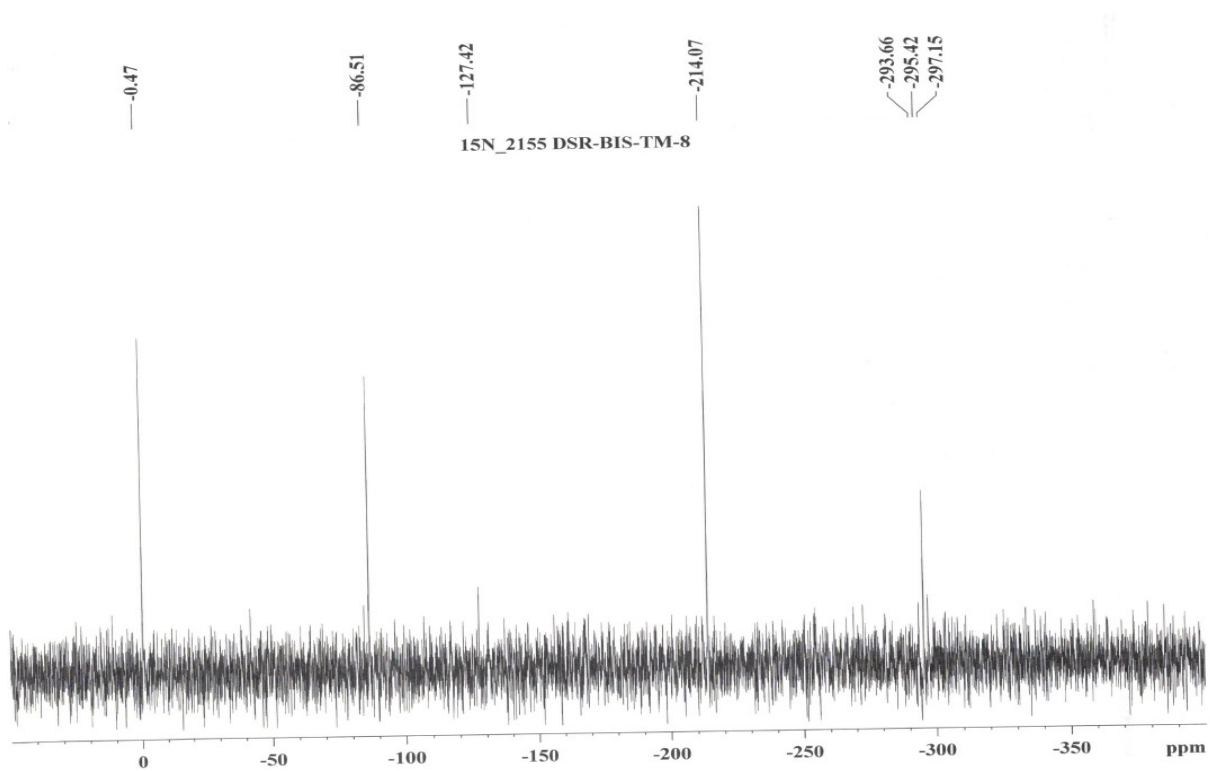


**Figure S25:** <sup>15</sup>N NMR spectrum of **7**.

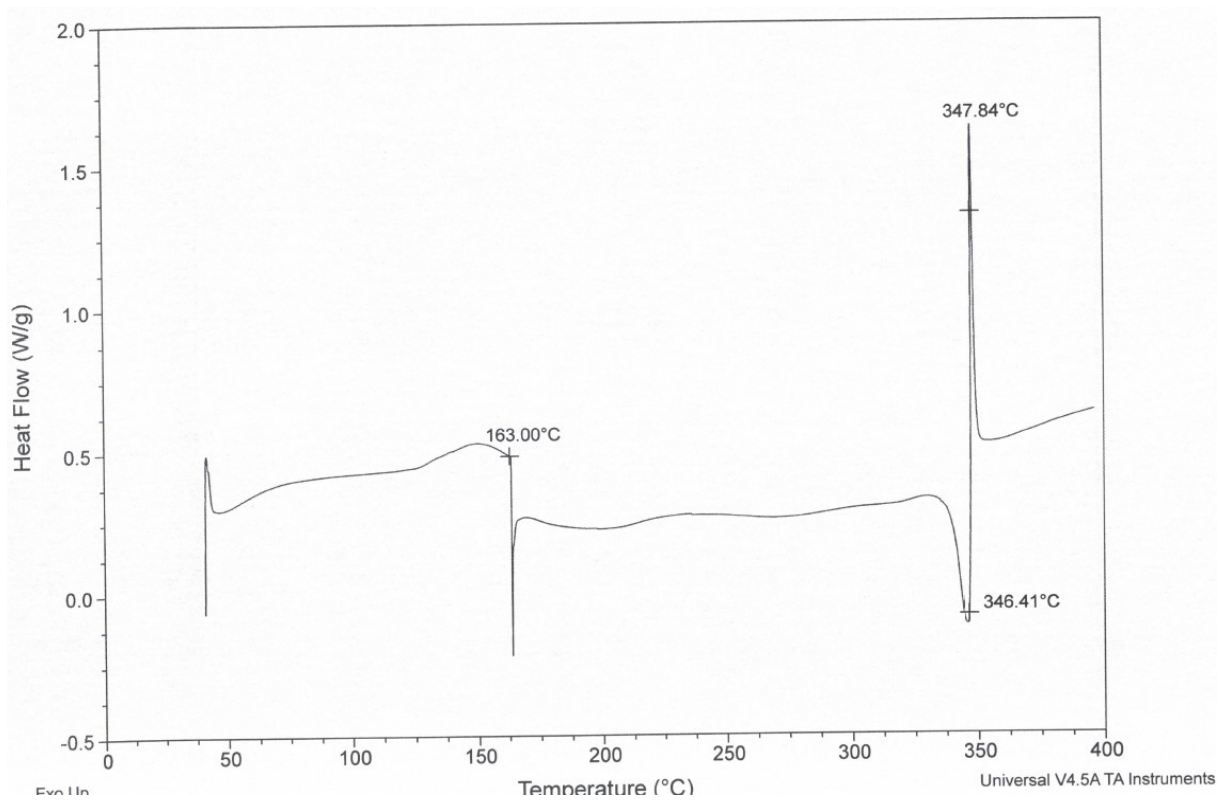


**Figure S26:** DSC plot of **7**.

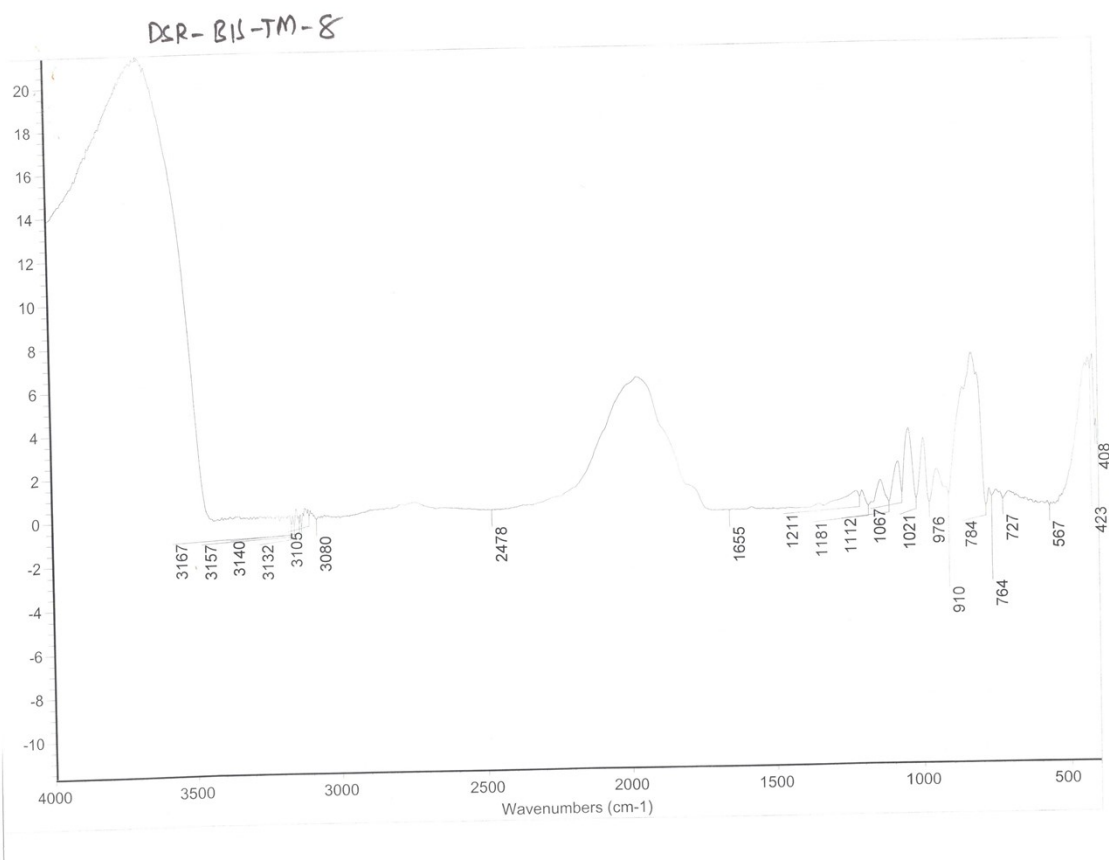


**Figure S27:** IR spectrum of 7.

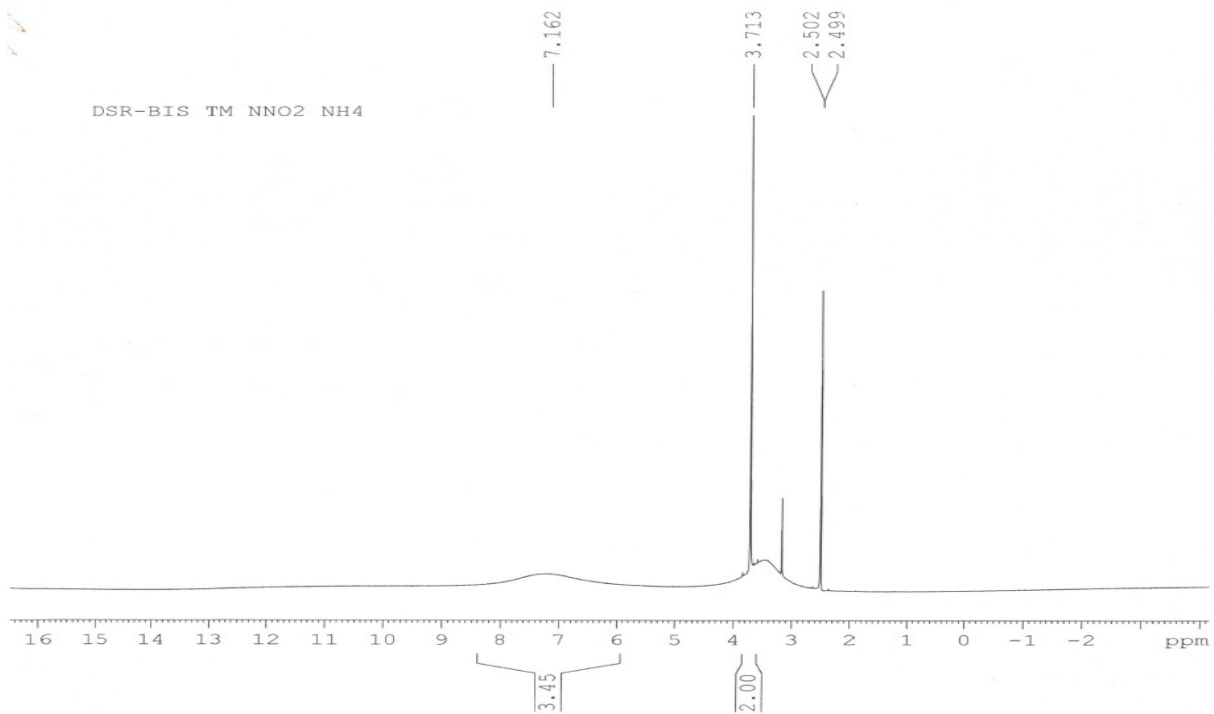


**Figure S28:**  $^1\text{H}$  NMR spectrum of **10**.

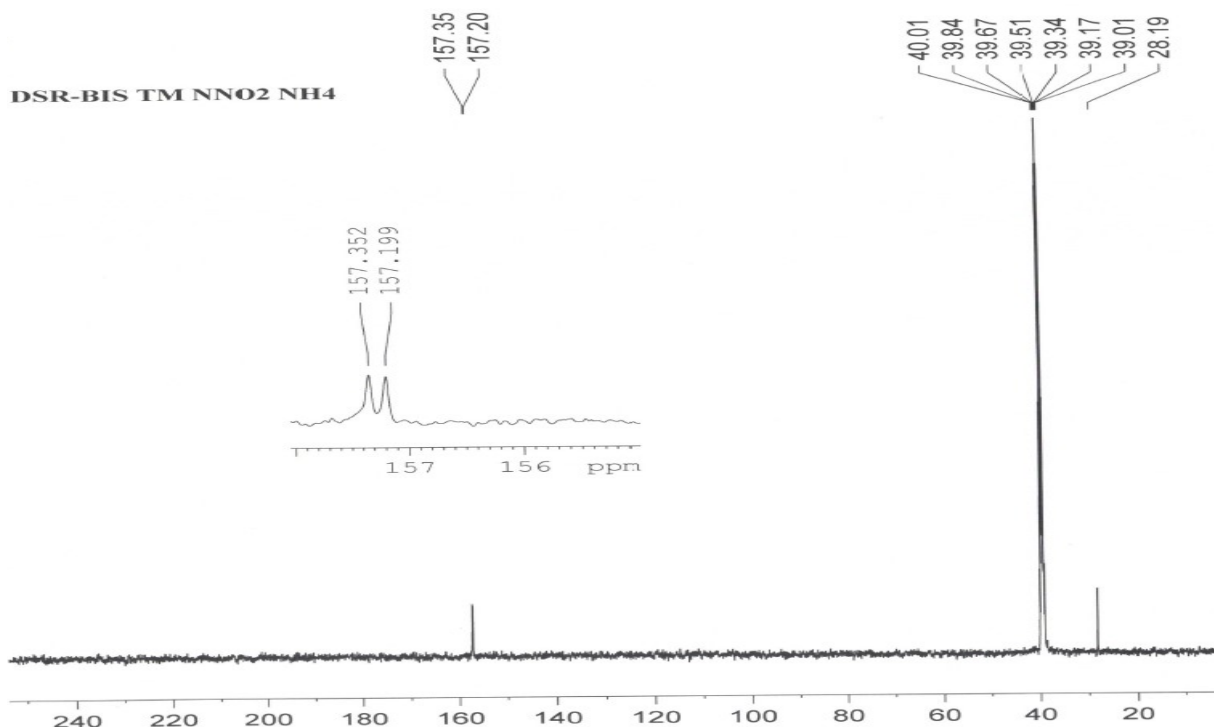


**Figure S29:**  $^{13}\text{C}$  NMR spectrum of **10**.

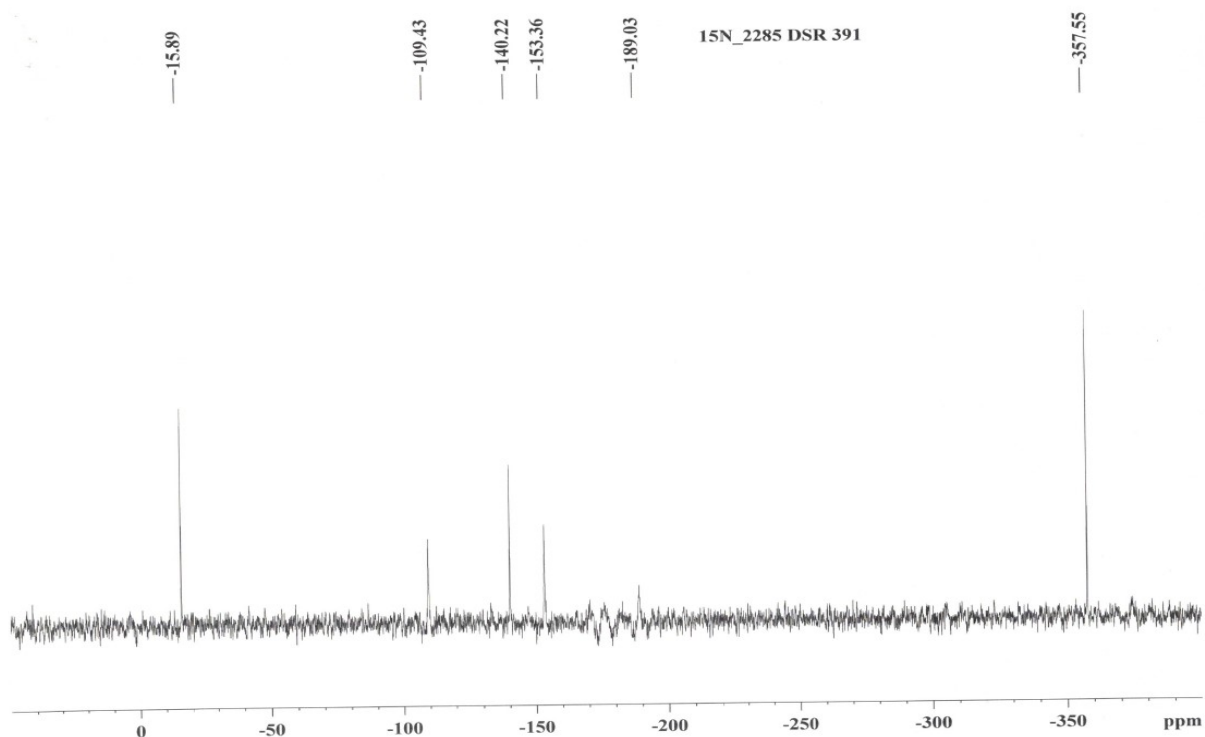


**Figure S30:**  $^{15}\text{N}$  NMR spectrum of **10**.

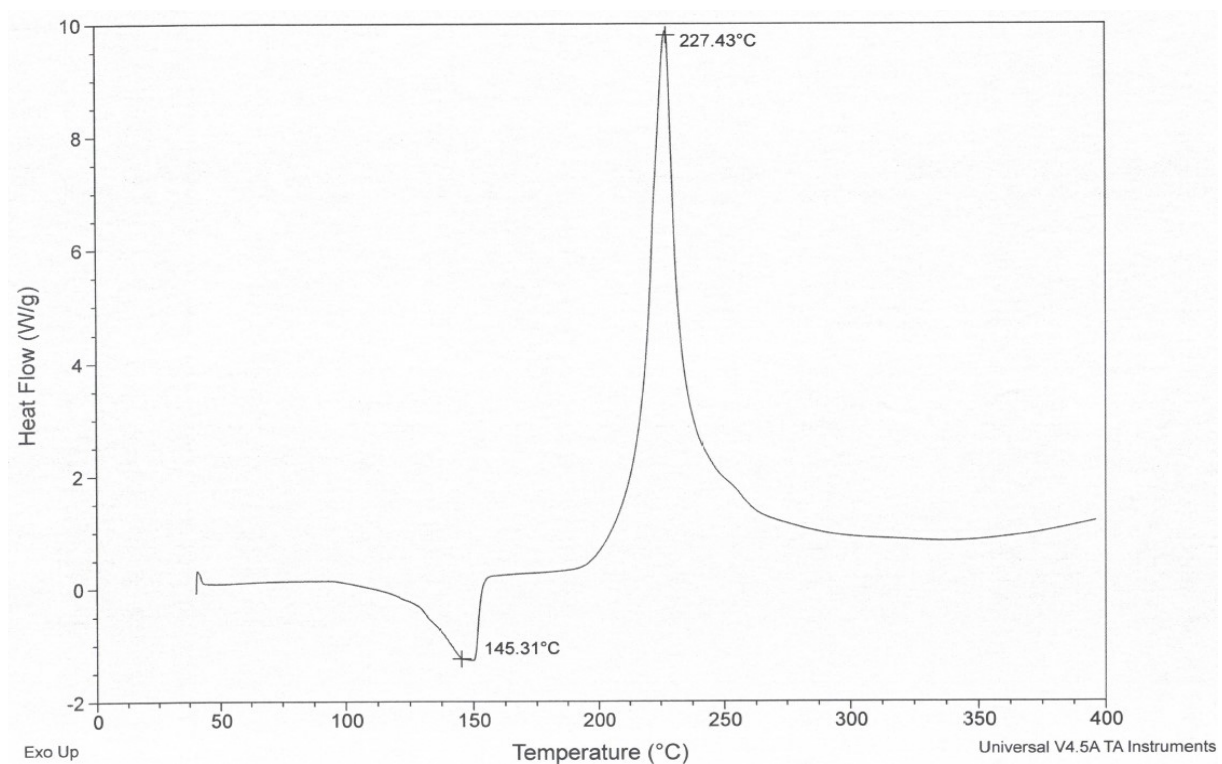


**Figure S31:** DSC plot of **10**.

DR-391

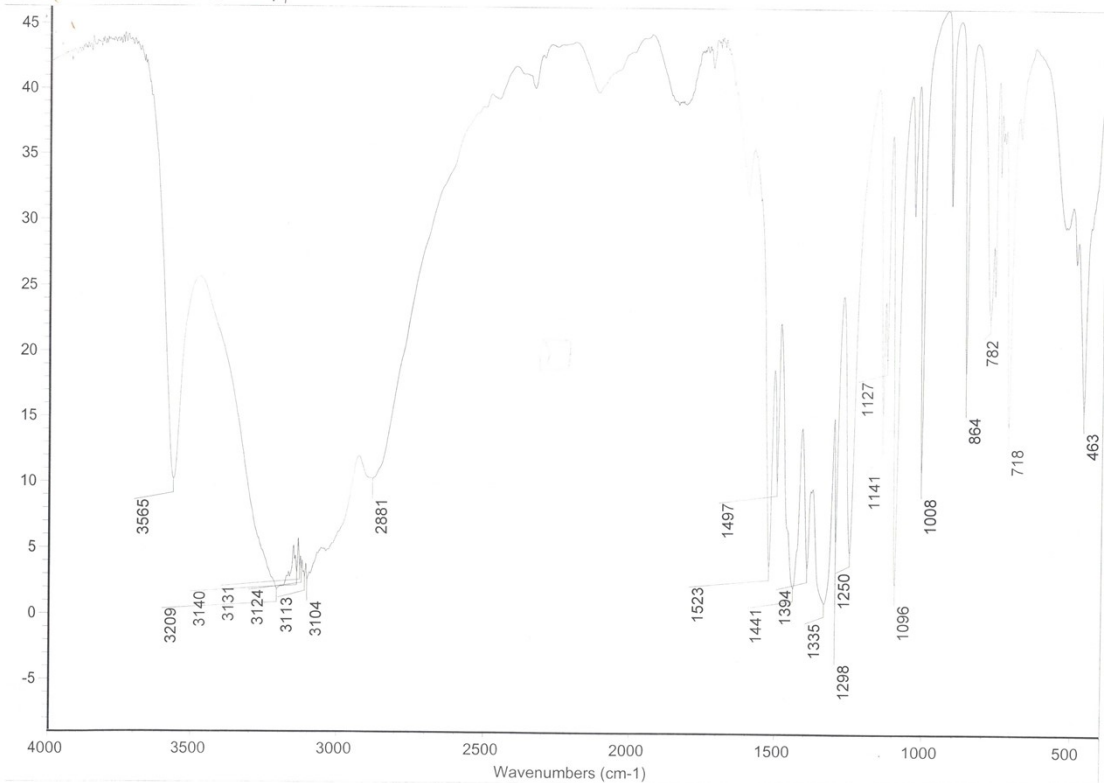


**Figure S32:** IR spectrum of **10**.

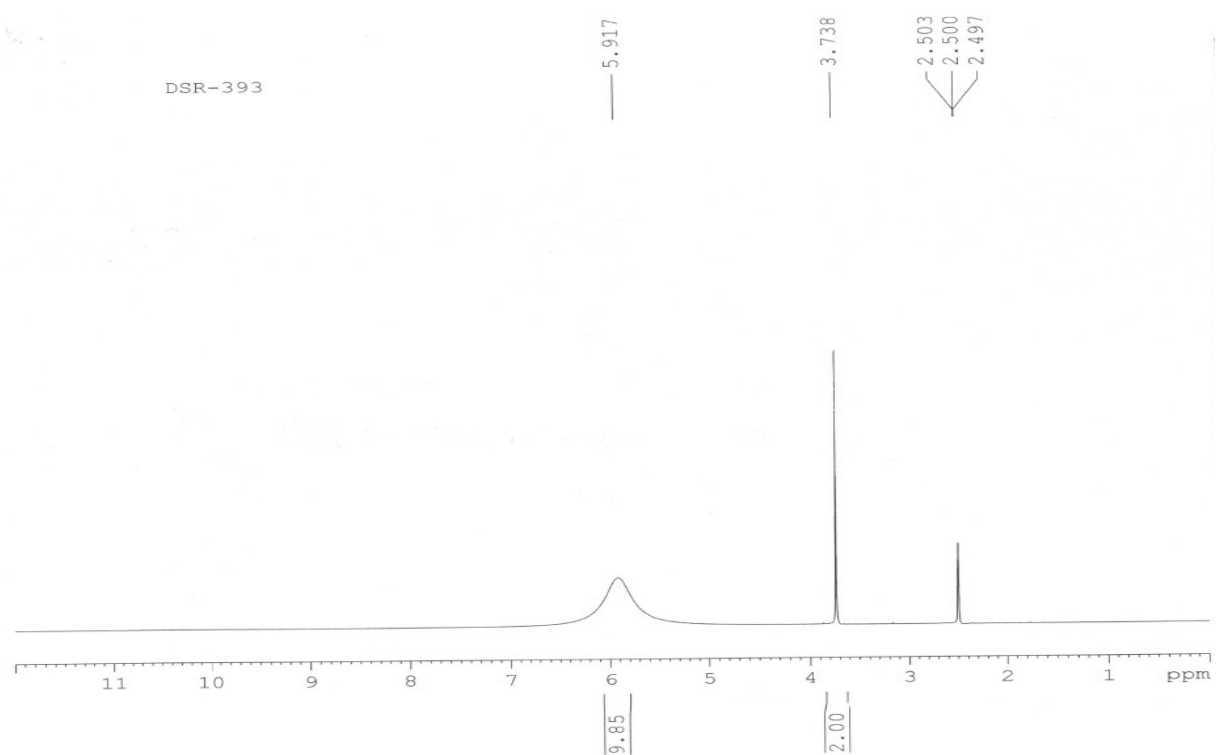


**Figure S33:** <sup>1</sup>H NMR spectrum of **11**.

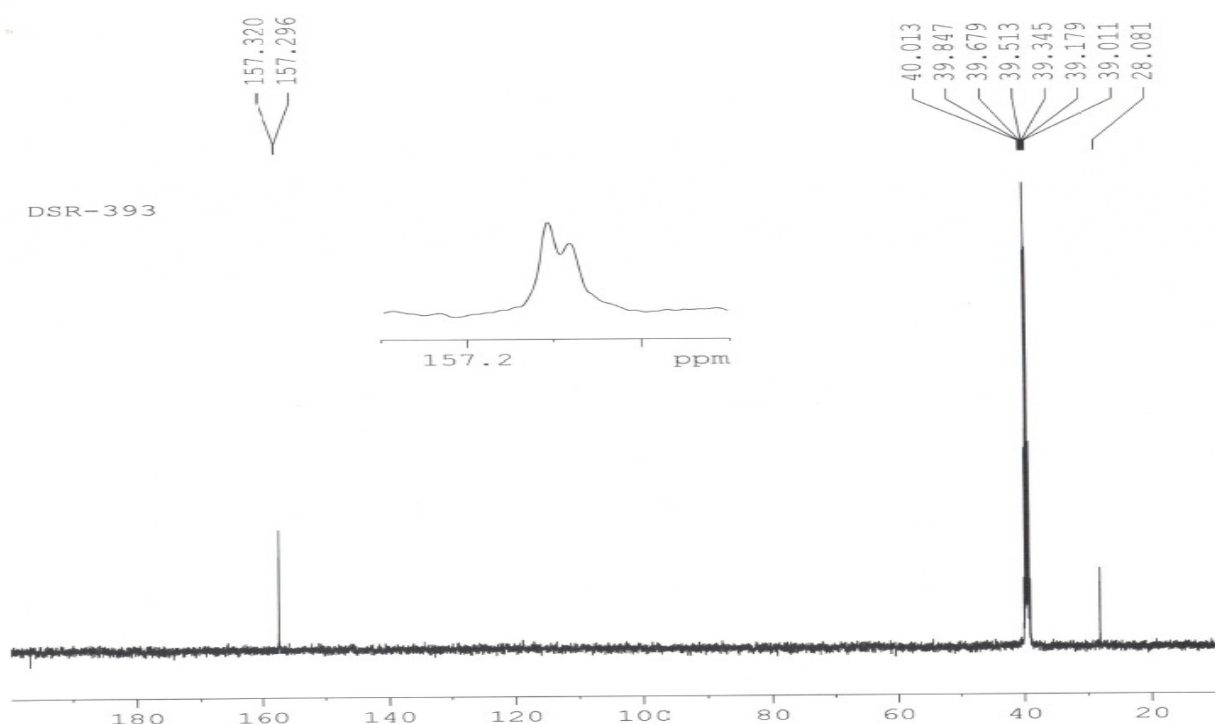


**Figure S34:** <sup>13</sup>C NMR spectrum of **11**.

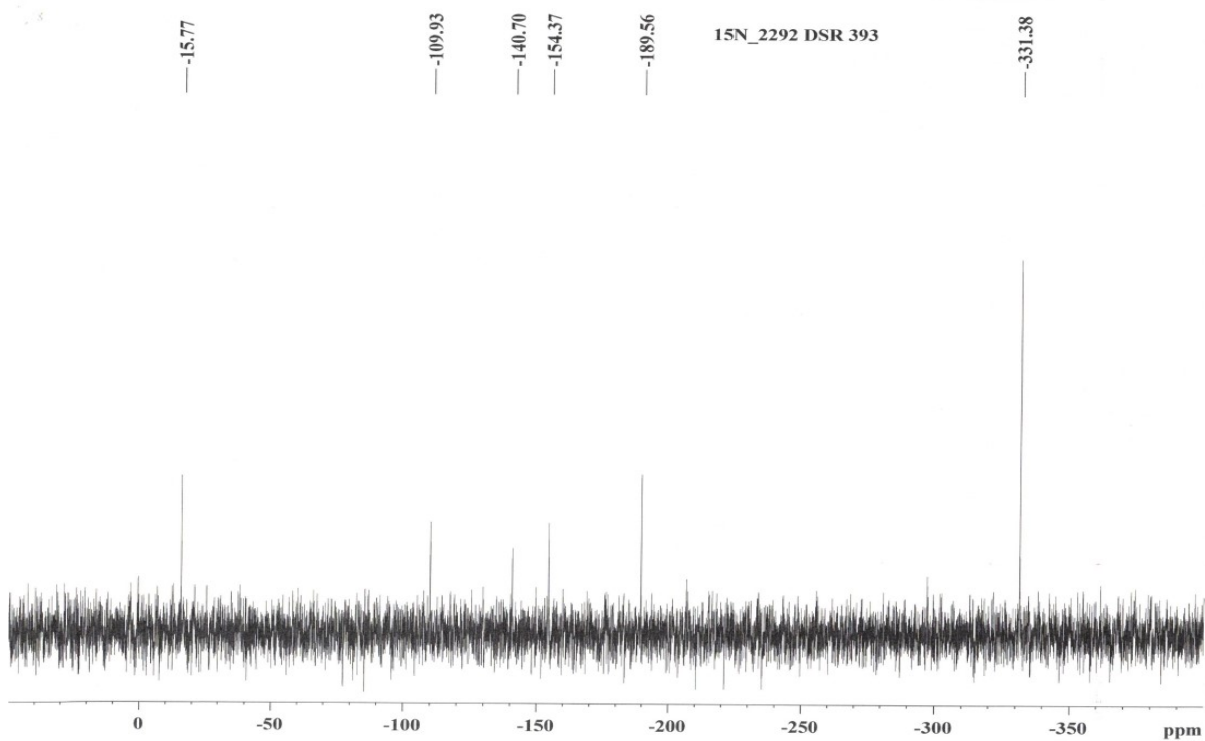


**Figure S35:** <sup>15</sup>N NMR spectrum of **11**.

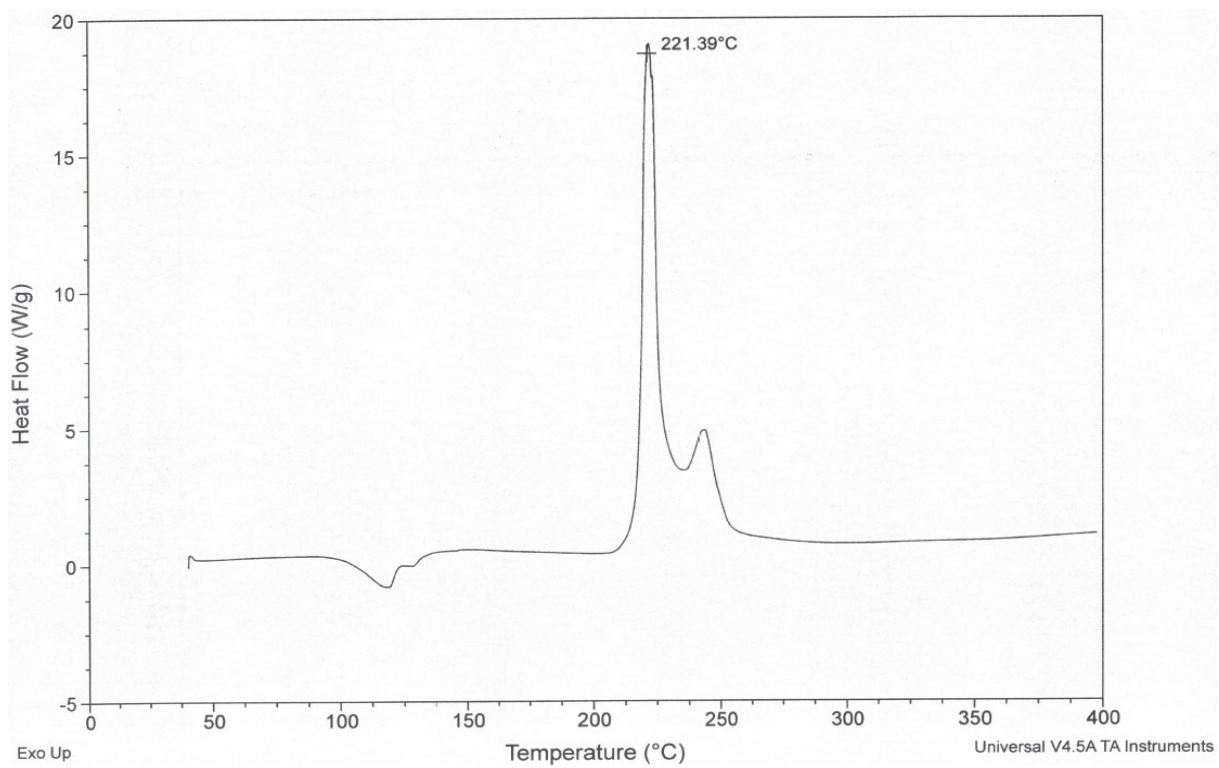


**Figure S36:** DSC plot of **11**.

DSR- 393

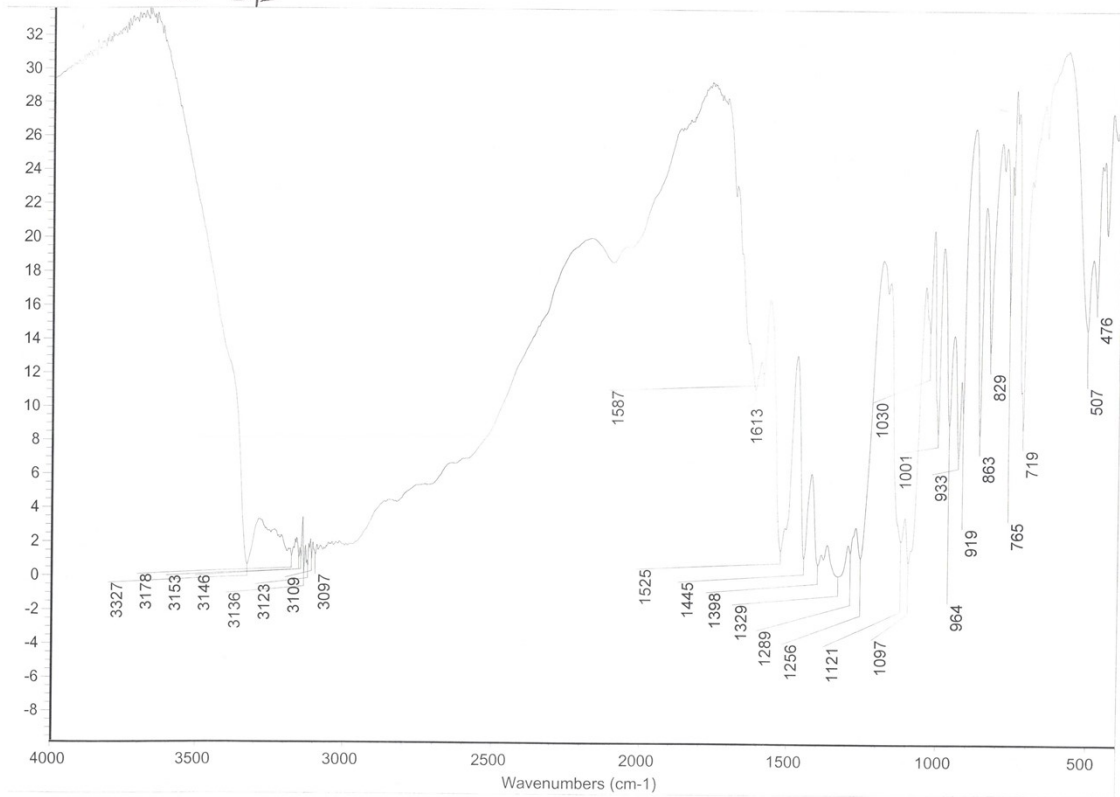


**Figure S37:** IR spectrum of **11**.

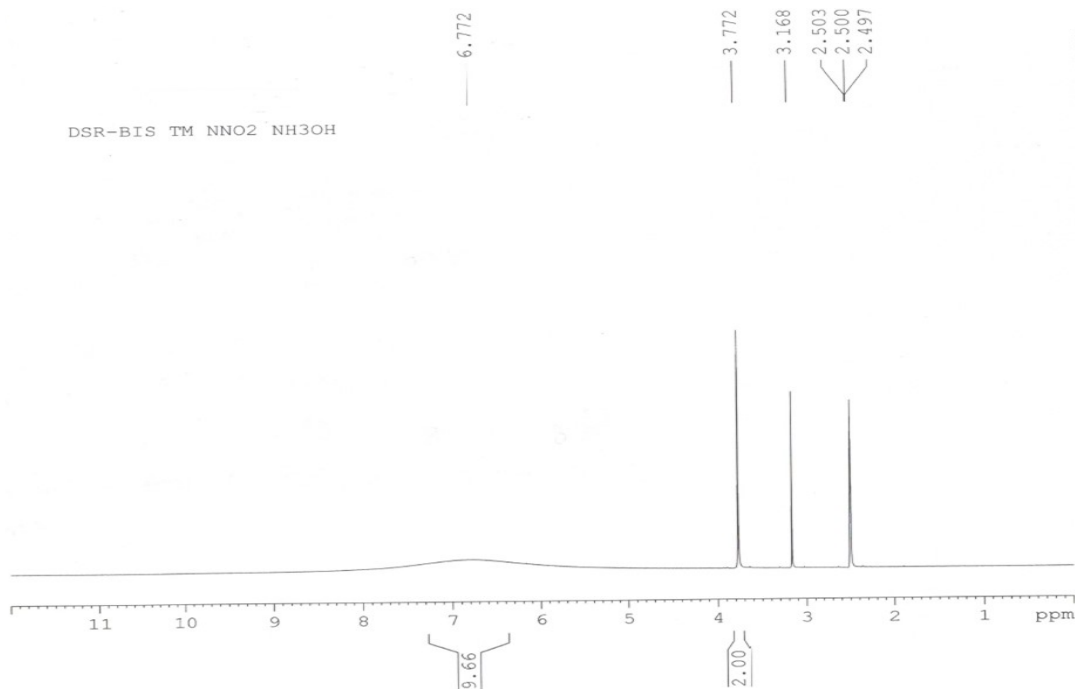


**Figure S38:**  $^1\text{H}$  NMR spectrum of **12**.

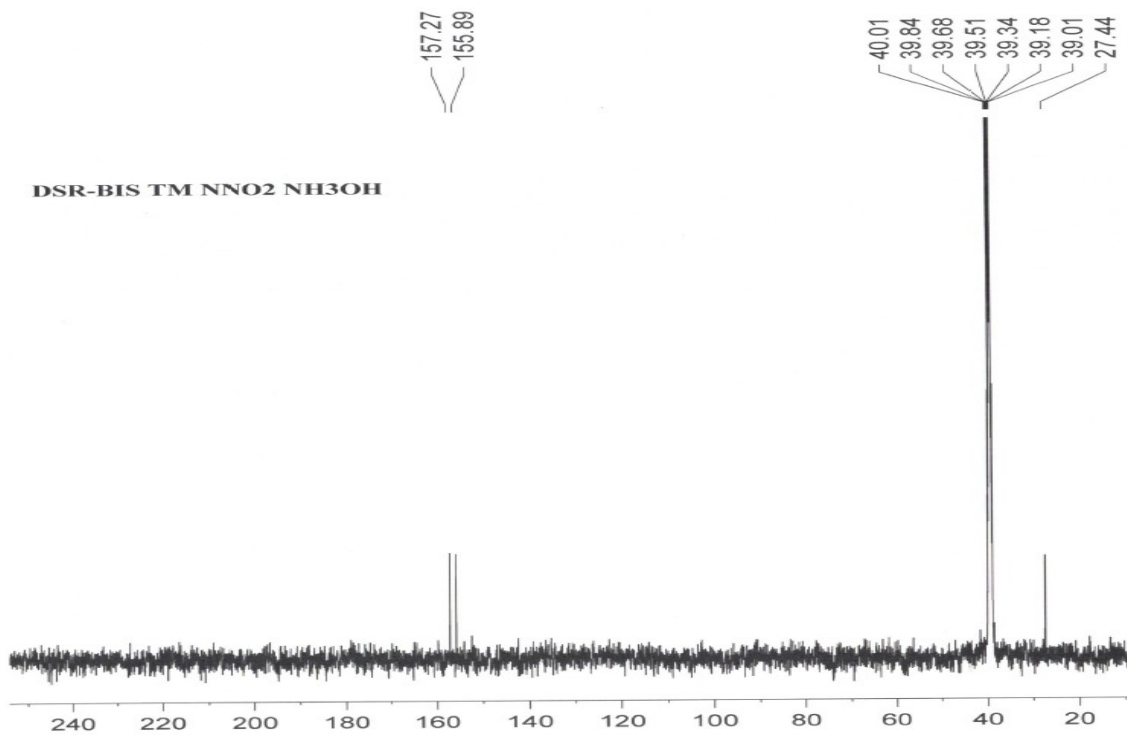


**Figure S39:**  $^{13}\text{C}$  NMR spectrum of **12**.

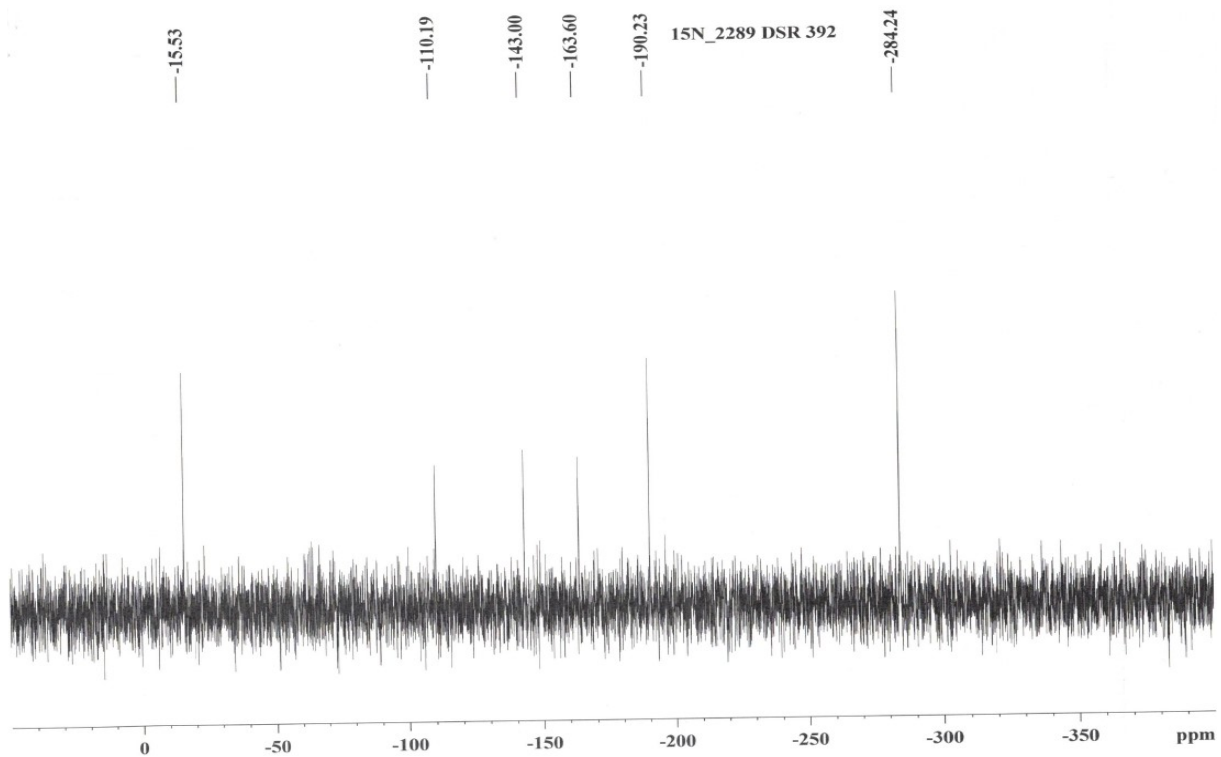


**Figure S40:** <sup>15</sup>N NMR spectrum of **12**.

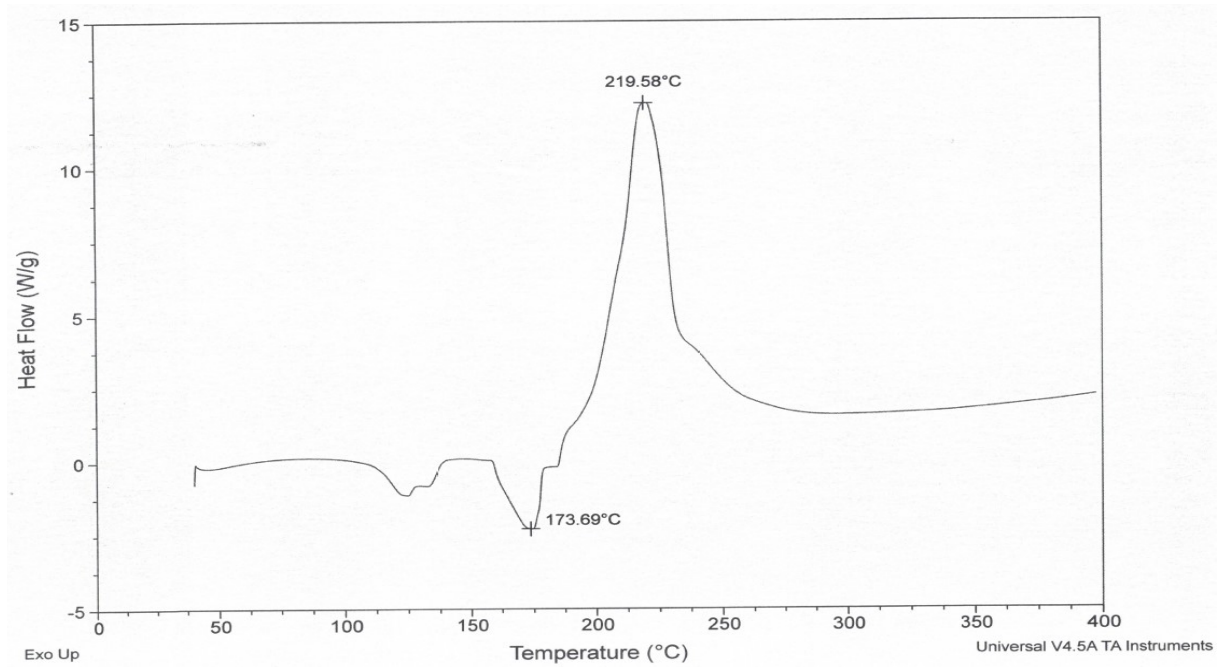


**Figure S41:** DSC plot of **12**.

DSR - 392

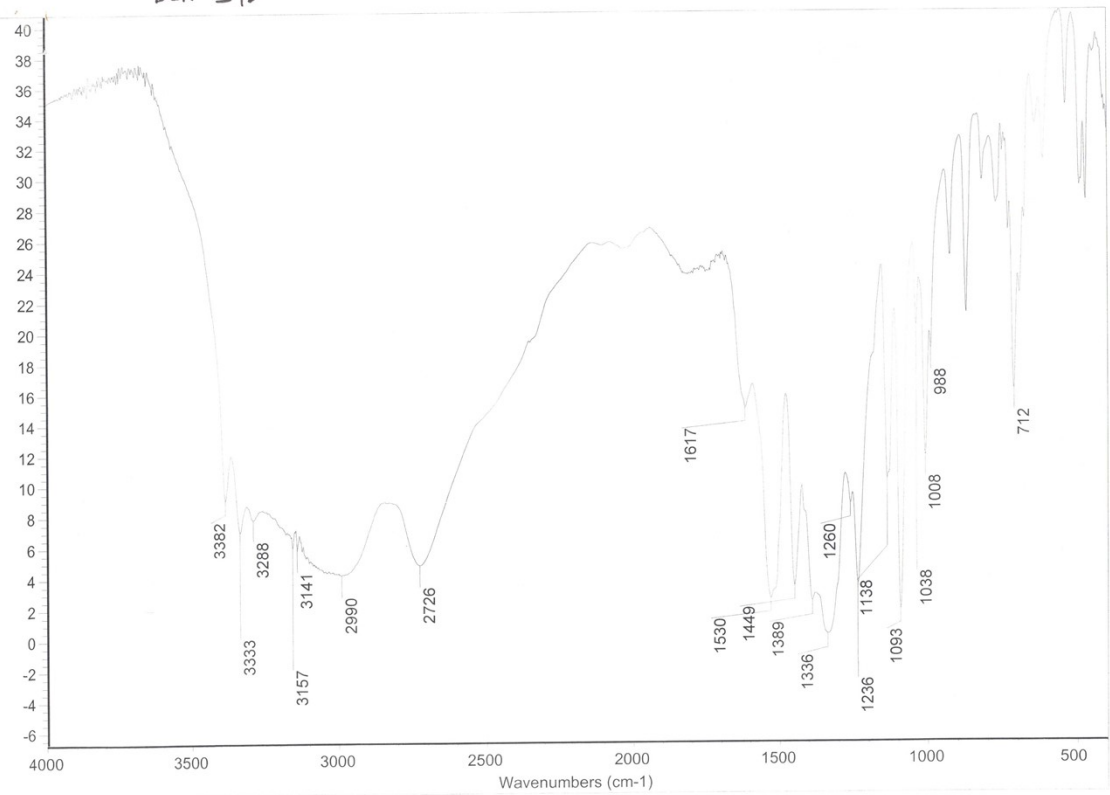


**Figure S42:** IR spectrum of **12**.

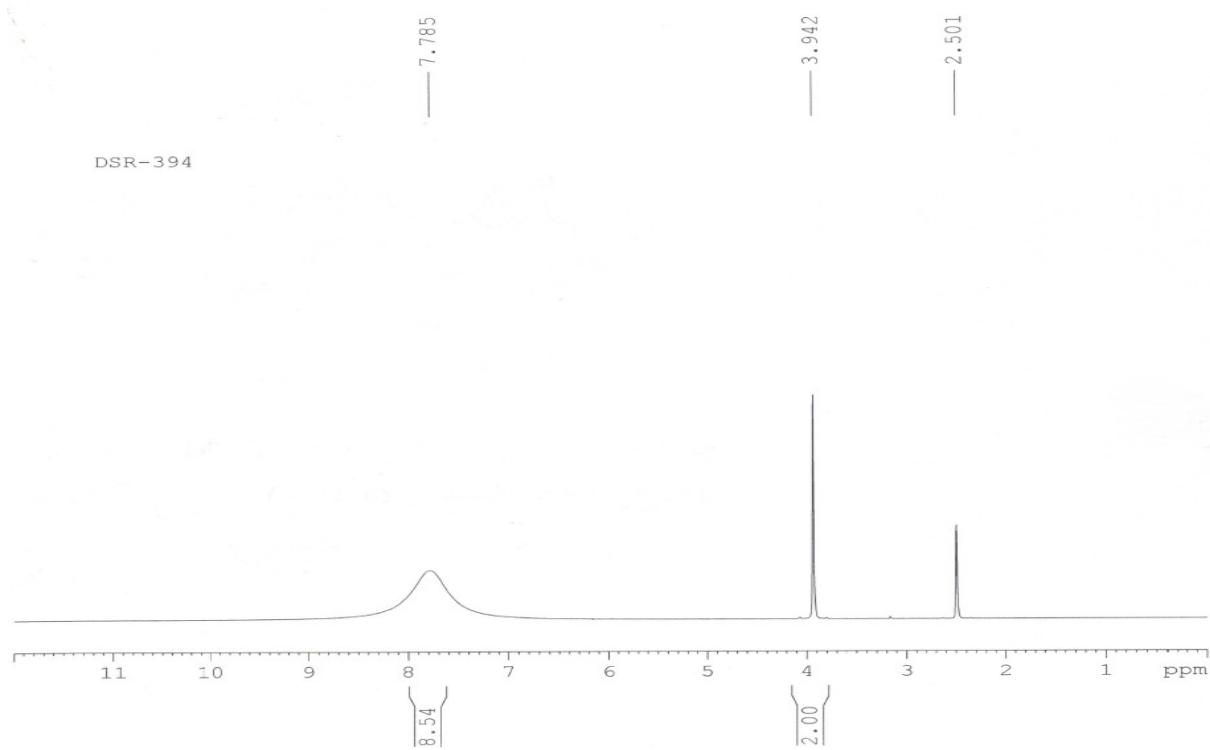


**Figure S43:** <sup>1</sup>H NMR spectrum of **13**.

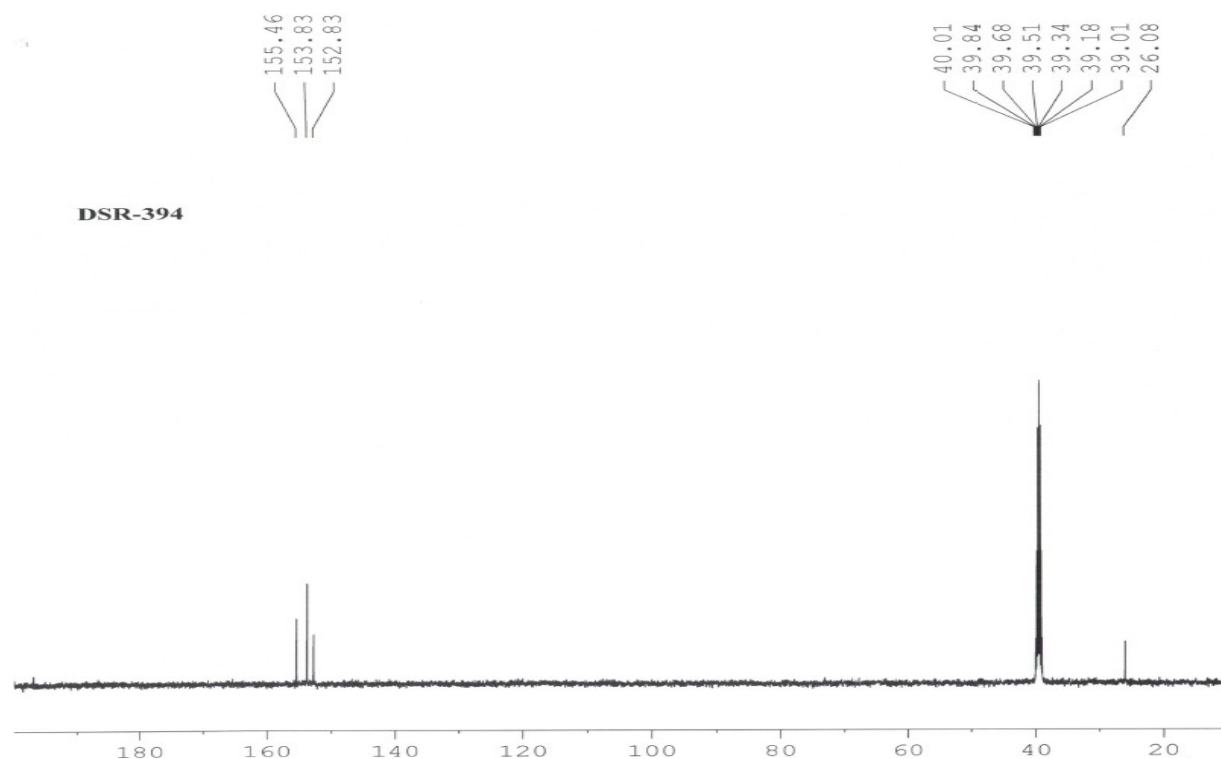


**Figure S44:** <sup>13</sup>C NMR spectrum of **13**.

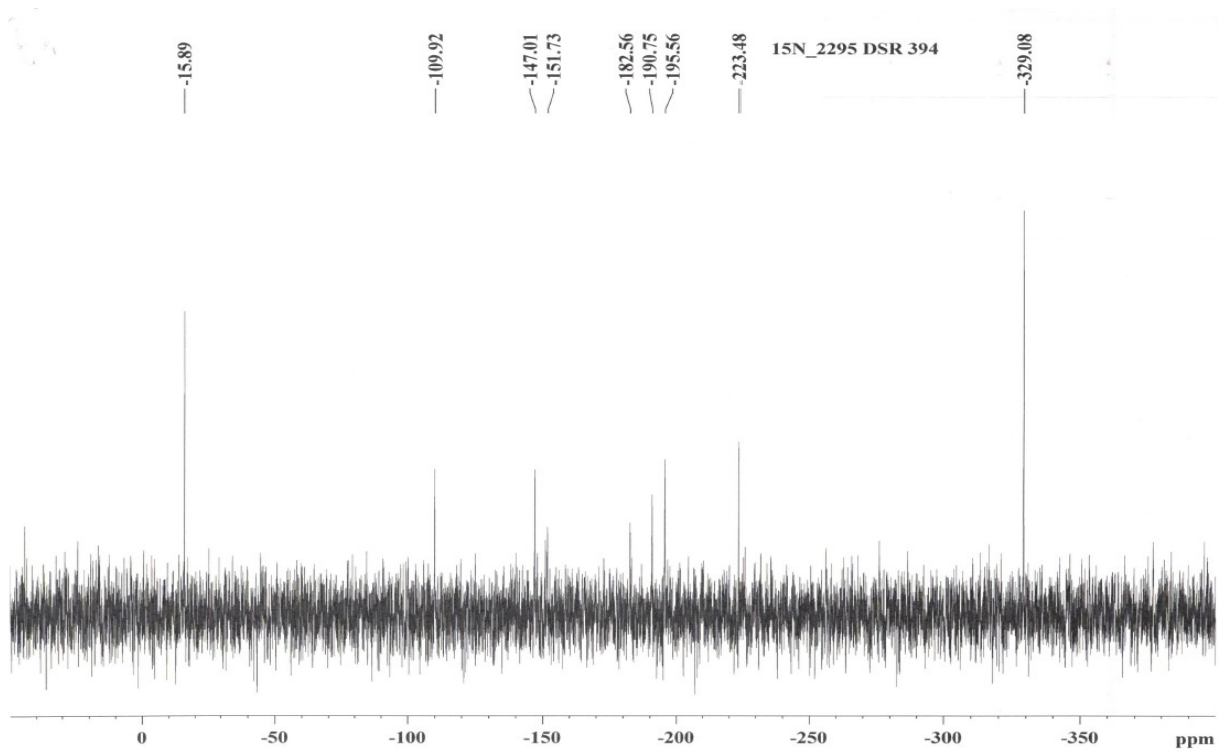


**Figure S45:** <sup>15</sup>N NMR spectrum of **13**.

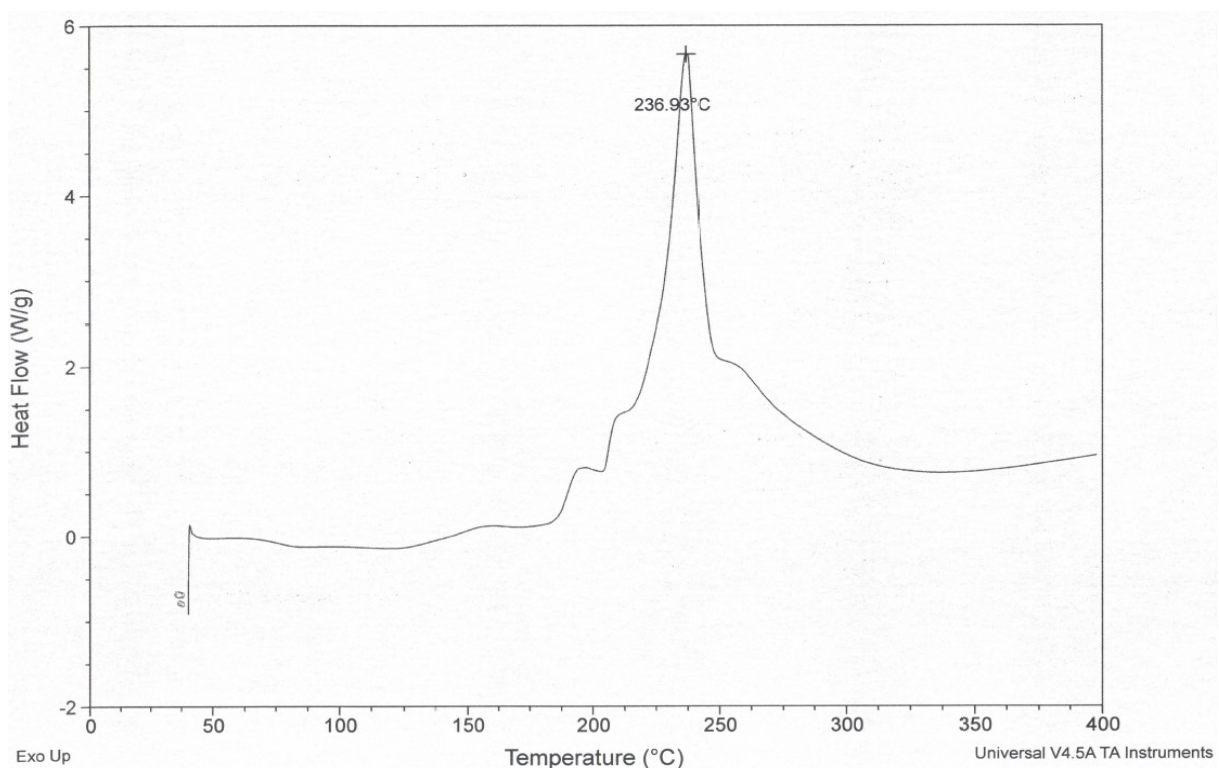


**Figure S46:** DSC plot of **13**.

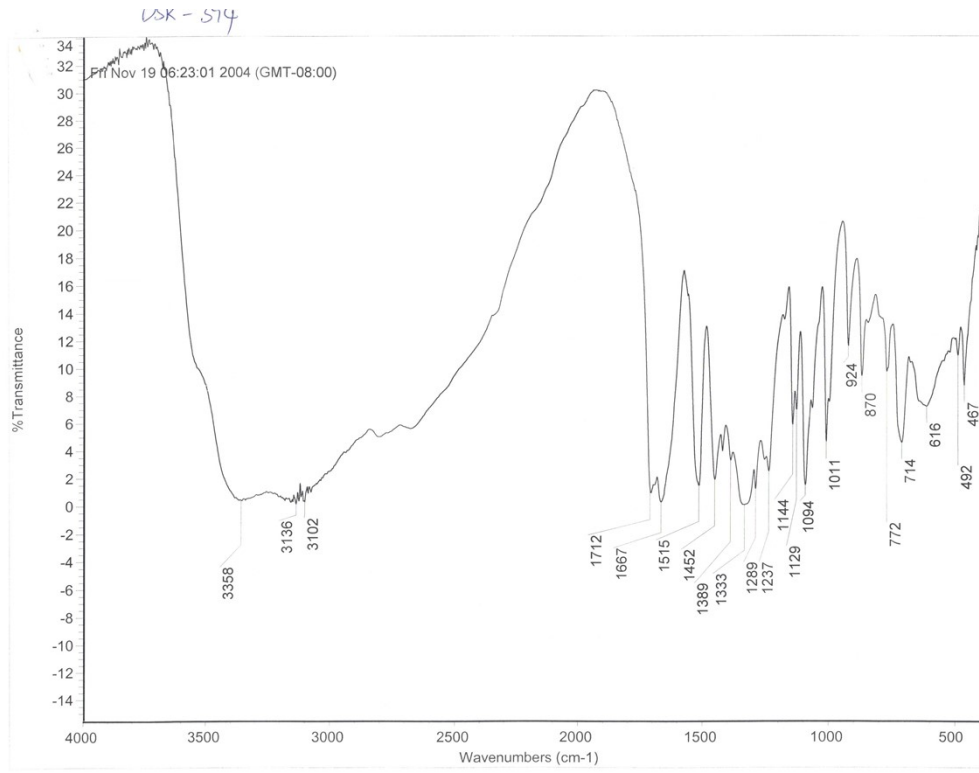


**Figure S47:** IR spectrum of **13**.

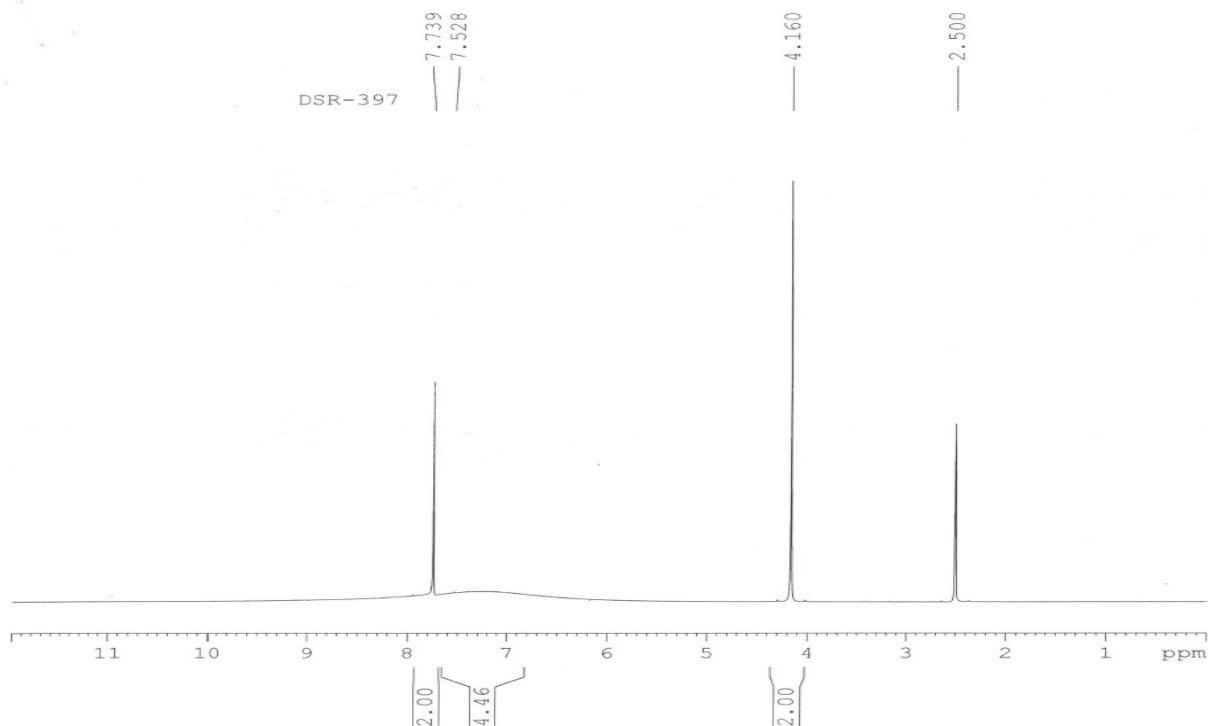


**Figure S48:**  $^1\text{H}$  NMR spectrum of **14**.

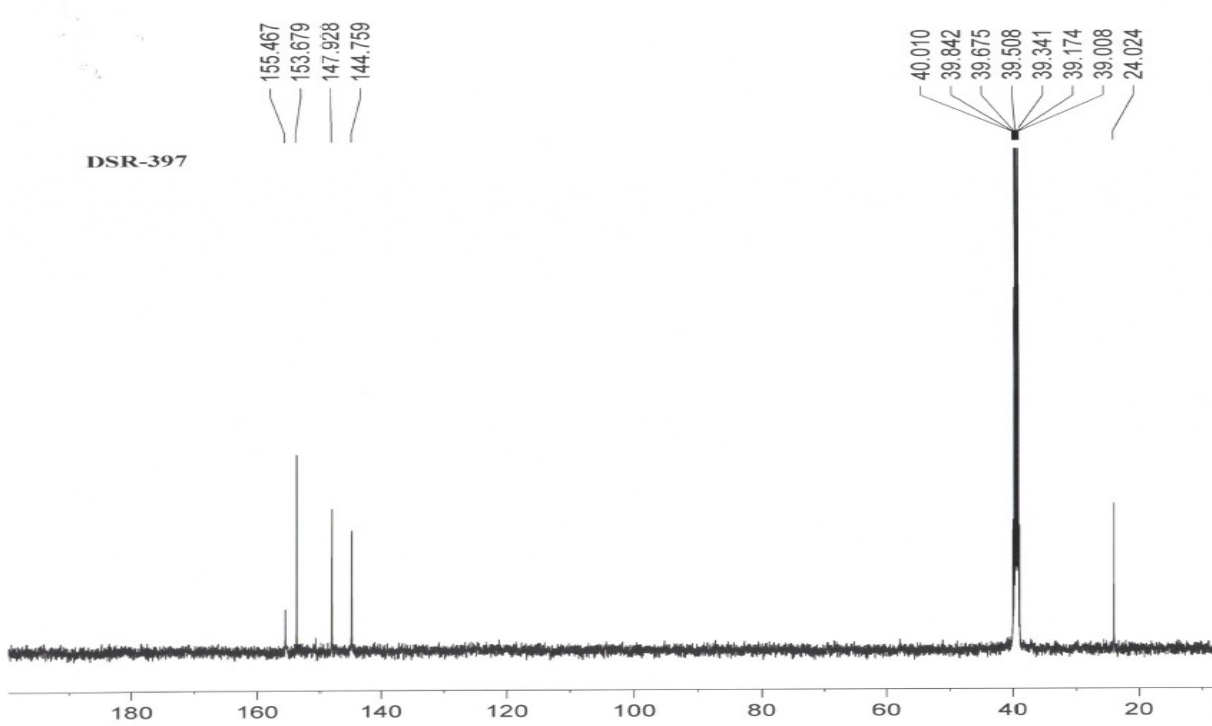


**Figure S49:**  $^{13}\text{C}$  NMR spectrum of **14**.

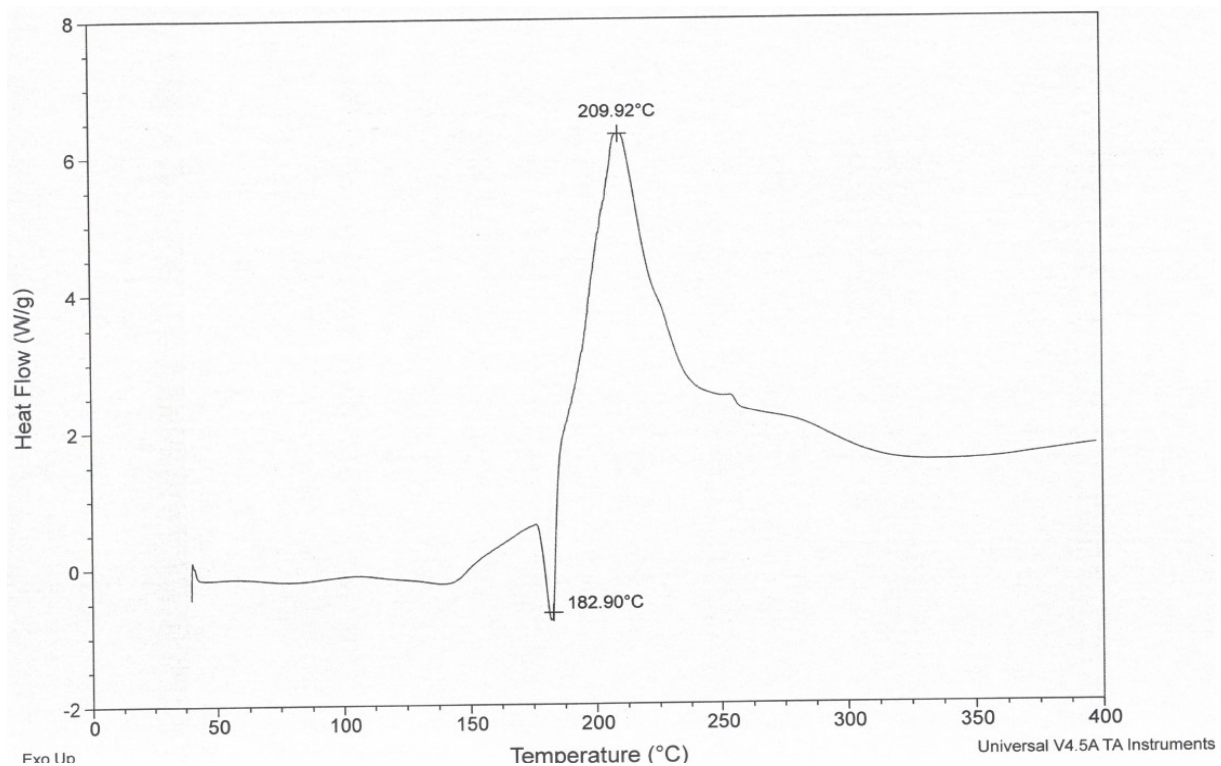


**Figure S50:** DSC plot of **14**.

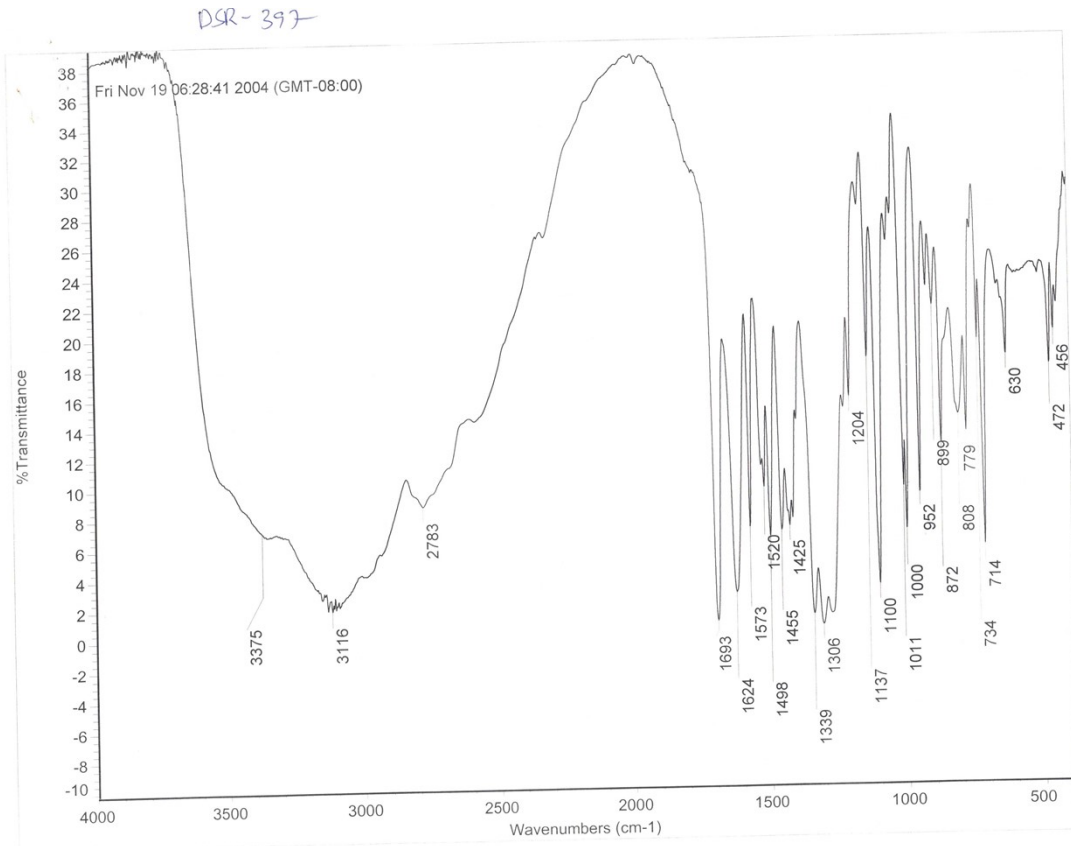


**Figure S51:** IR spectrum of **14**.

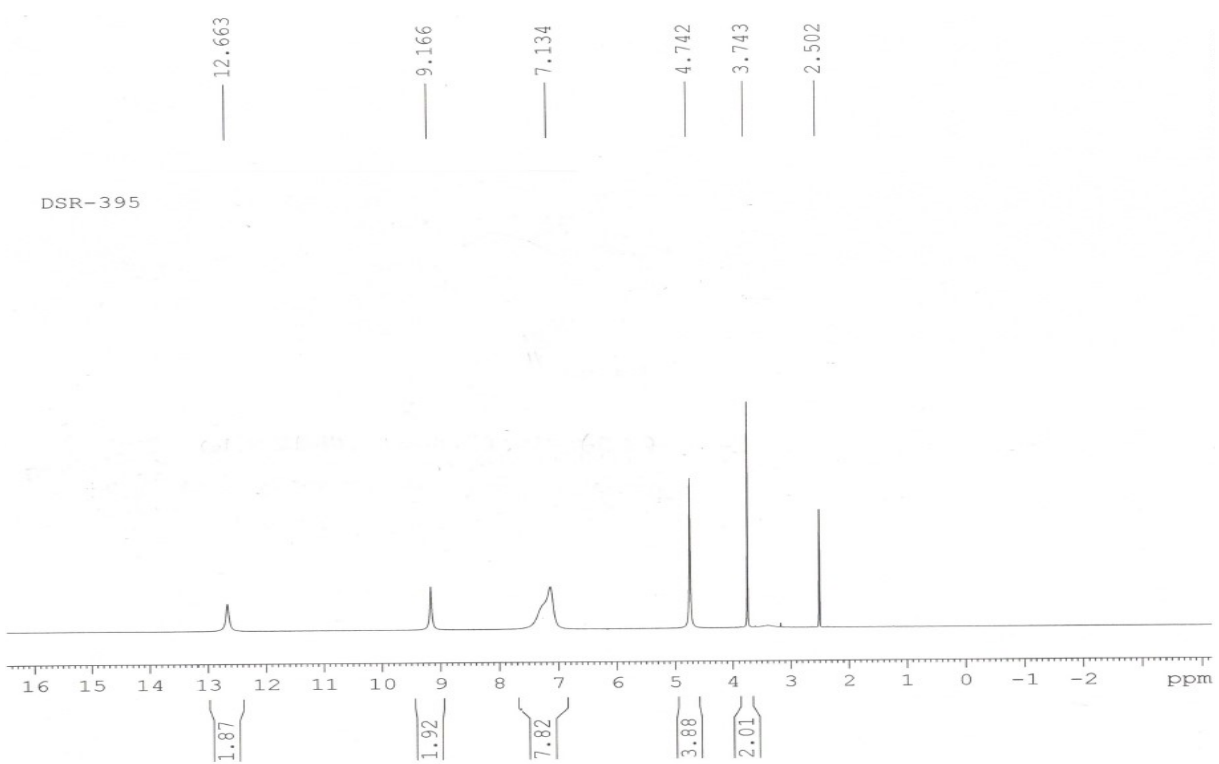


**Figure S52:**  $^1\text{H}$  NMR spectrum of **15**.

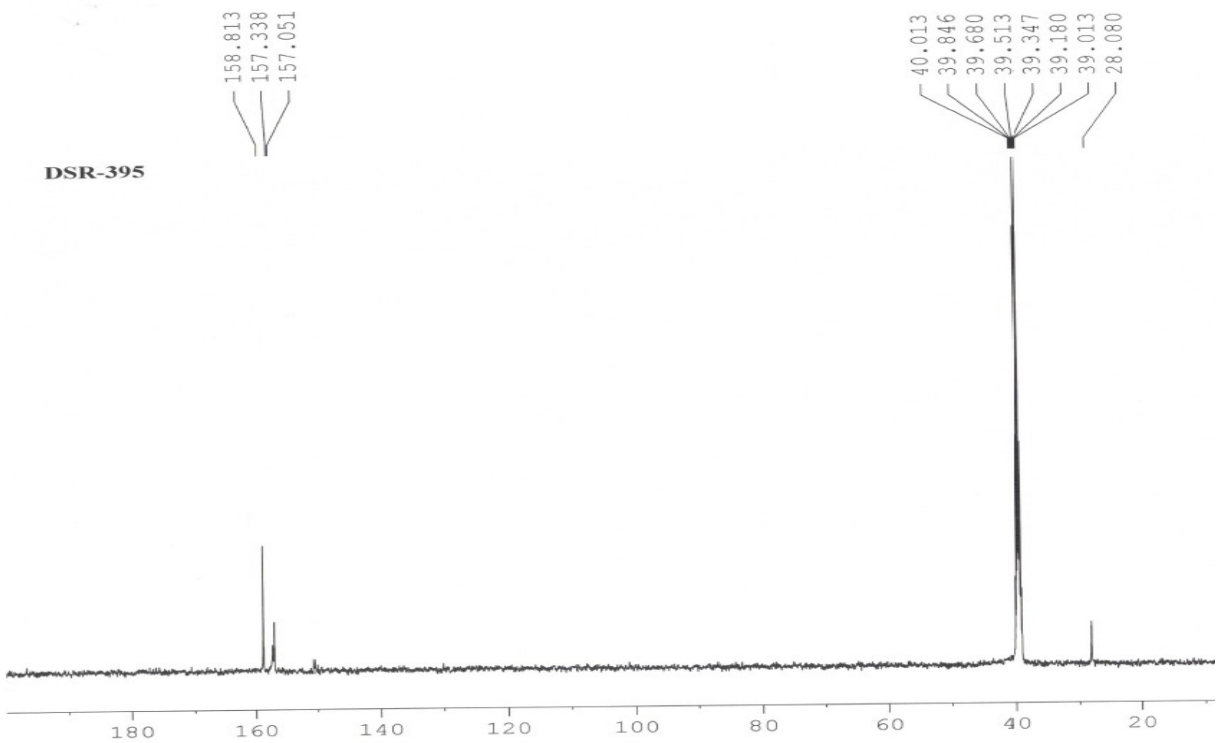


**Figure S53:**  $^{13}\text{C}$  NMR spectrum of **15**.

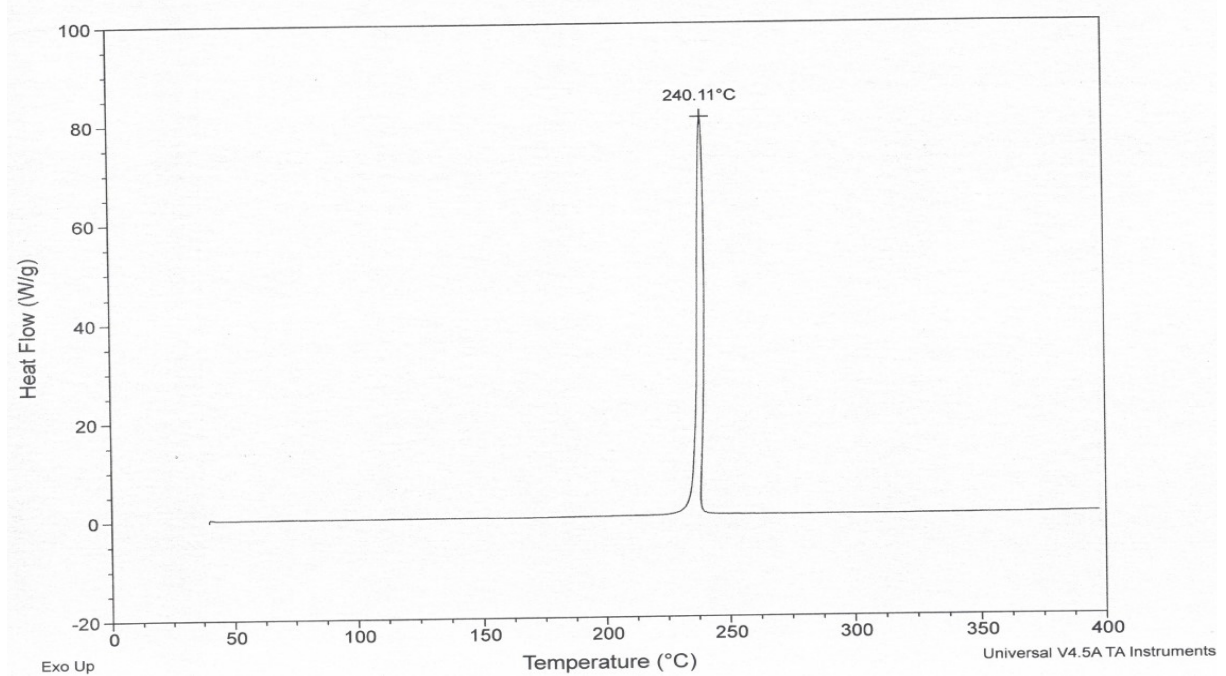


**Figure S54:** DSC plot of **15**.

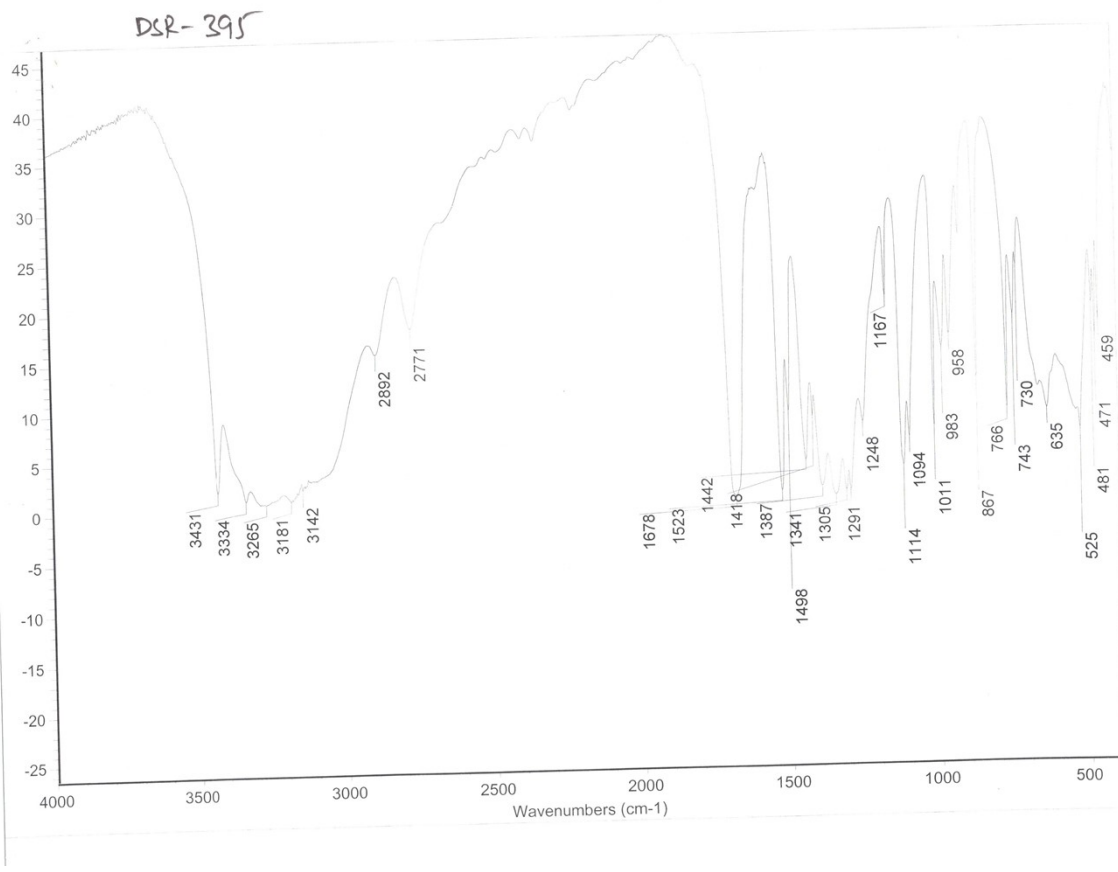


**Figure S55:** IR spectrum of **15**.

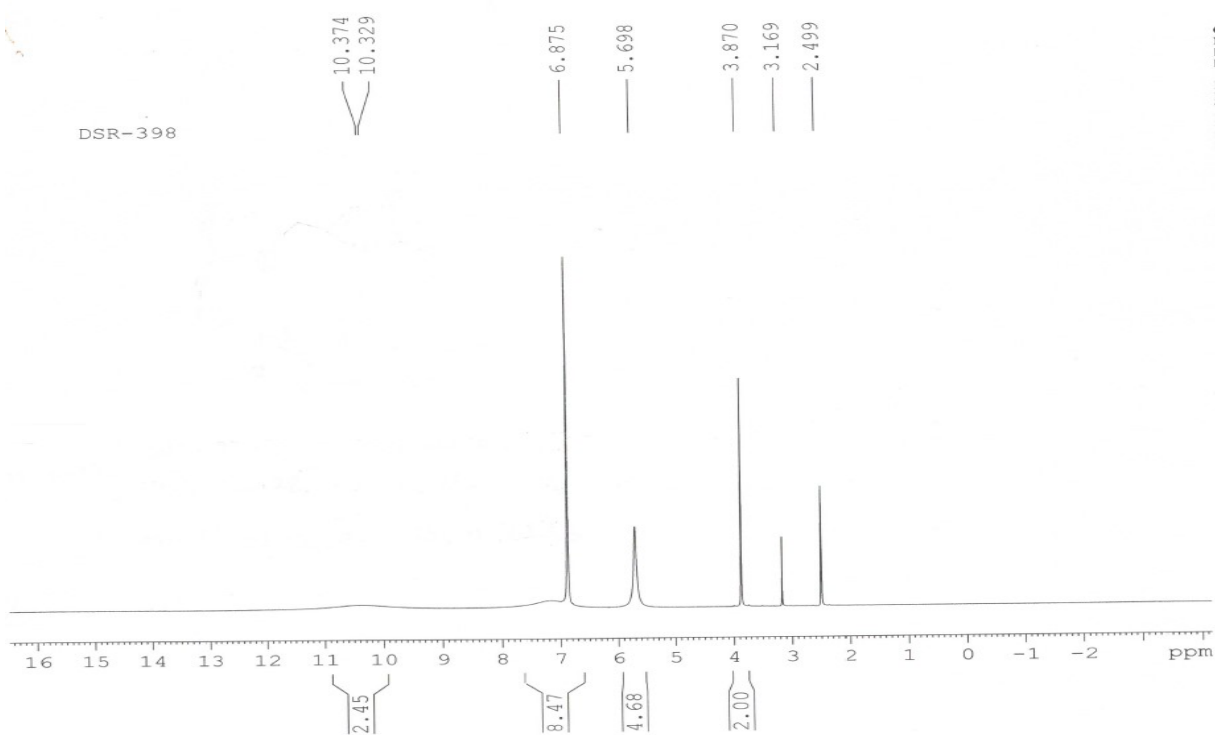


**Figure S56:**  $^1\text{H}$  NMR spectrum of **16**.

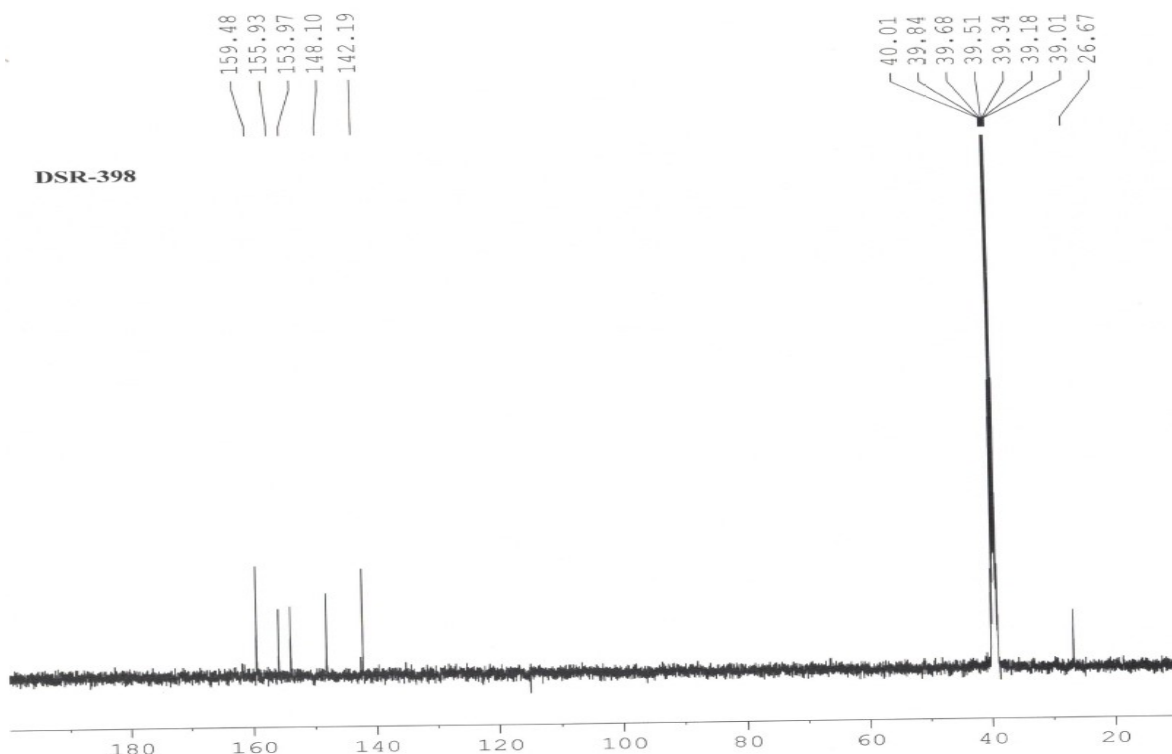


**Figure S57:**  $^{13}\text{C}$  NMR spectrum of **16**.

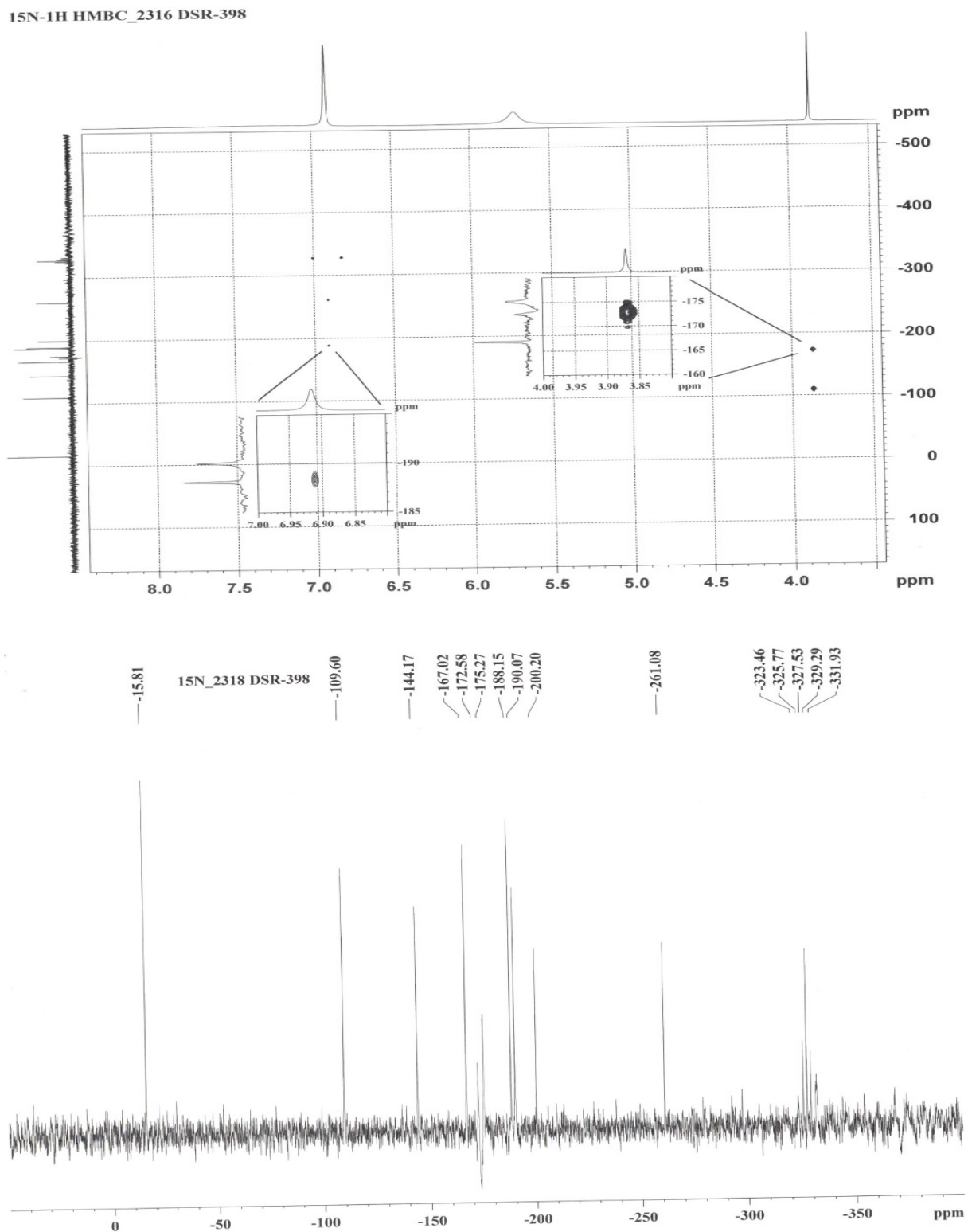


**Figure S58:**  $^{15}\text{N}$  NMR spectrum of **16**.

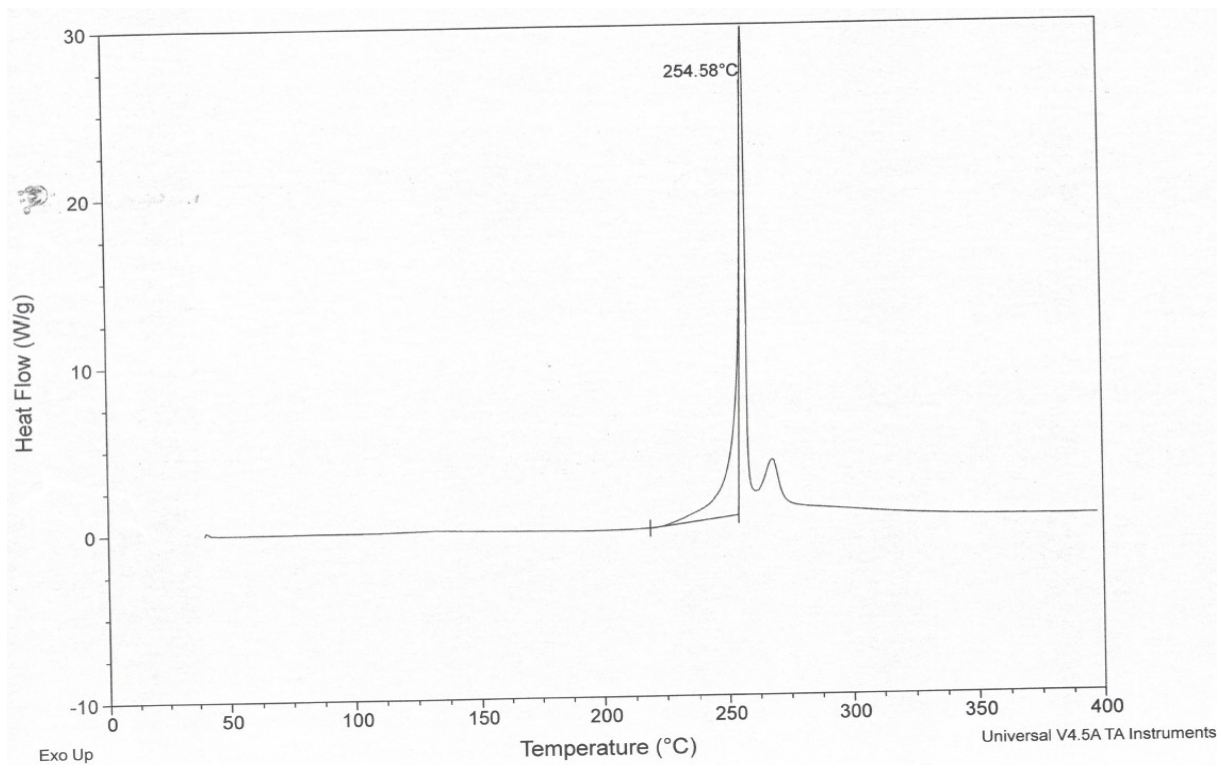


**Figure S59:** DSC plot of **16**.

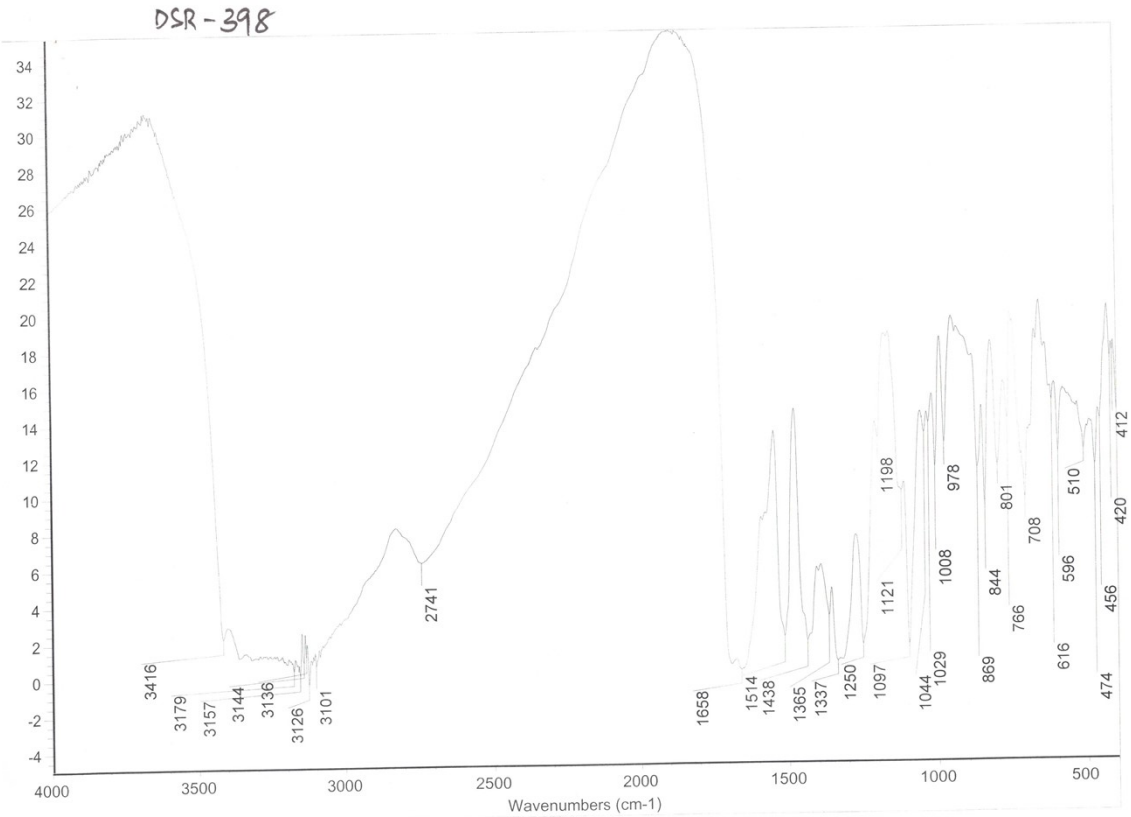


**Figure S60:** IR spectrum of **16**.

### Computational Methods:

Computations were carried out using the Gaussian 09 program suite.<sup>3</sup> The structure optimizations are performed with B3PW91 functional with 6-31G(d,p) basis set and characterized to be true local energy minima on the potential energy surface and no imaginary frequencies were found. Isodesmic reactions have been designed to predict the gas phase HOF ( $\text{HOF}_{\text{gas}}$ ). The usage of  $\text{HOF}_{\text{gas}}$  in the calculation of detonation properties slightly

overestimates the values of detonation velocity and detonation pressure, and hence, the solid phase HOF ( $\text{HOF}_{\text{solid}}$ ) can effectively reduce the errors. The  $\text{HOF}_{\text{solid}}$  is calculated as the difference between  $\text{HOF}_{\text{gas}}$  and heat of sublimation ( $\text{HOF}_{\text{sub}}$ ) as,

$$\text{HOF}_{\text{solid}} = \text{HOF}_{\text{gas}} - \text{HOF}_{\text{sub}} \quad (1)$$

$\text{HOF}_{\text{sub}}$  depend on the molecular surface properties and calculated using equation (2) proposed by Politzer et al.<sup>4</sup>

$$\text{HOF}_{\text{sub}} = 4.4307 \times 10^{-4} A^2 + 2.0599(v\sigma_{\text{tot}}^2)^{0.5} - 2.4825 \quad (2)$$

where  $A$  represent the surface area of the 0.001 electrons/bohr<sup>3</sup> isosurface of electronic density,  $v$  denotes the degree of balance between the positive and negative surface potentials, and  $\sigma_{\text{tot}}^2$  is the electrostatic potential variance. The molecular surface properties were obtained using the Multiwfn program.<sup>5</sup> The HOF of energetic salts were predicted using Born–Haber cycle (Figure S2) and can be simplified by the equation (3),

$$\text{HOF}(\text{salt}, 298 \text{ K}) = \text{HOF}(\text{cation}, 298 \text{ K}) + \text{HOF}(\text{anion}, 298 \text{ K}) - H_L \quad (3)$$

in above equation,  $H_L$  is the lattice energy of the salts, which can be predicted by using the formula proposed by Jenkins et al.<sup>6</sup>

$$H_L = U_{\text{POT}} + [p(\frac{n_M}{2} - 2) + q(\frac{n_X}{2} - 2)]RT \quad (4)$$

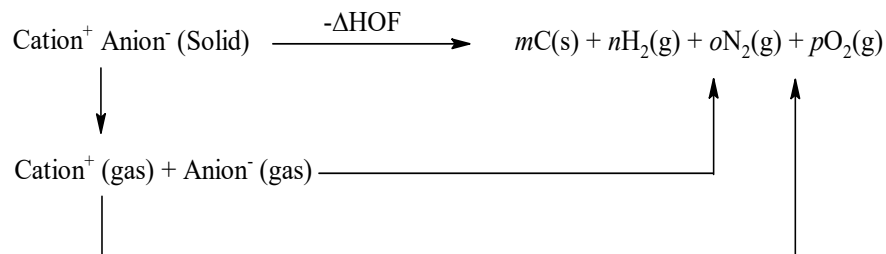


**Figure S2.** Born-Haber cycle for the formation of energetic salts.

The nature of the cation  $M_p^+$  and anion  $X_q^-$  decide  $n_M$  and  $n_X$  values, respectively and are equal to three for monoatomic ions, five for linear polyatomic ions, and six for nonlinear polyatomic ions.  $U_{\text{POT}}$  is the lattice potential energy, calculated using the density ( $\rho$  in g/cm<sup>3</sup>) and the chemical formula mass (M in g/mol) of the ionic salt.

**Table S16.** Energy content data for salts 3-7.

Salt No.	Anion	2 X Cation	$\text{HOF}_{\text{cation}}$ (kJ/mol)	$\text{HOF}_{\text{anion}}$ (kJ/mol)	$U_{\text{POT}}$ (kJ/mol)	$H_L$ (kJ/mol)	$\text{HOF}_{\text{salt}}$ (kJ/mol)
3			877.6	714.5	1164.7	1177.2	1292
4			753.8	714.5	1207.9	1220.3	1001
5			954.4	714.5	1258.9	1271.3	1351
6			1019	714.5	1222.5	1234.9	1517
7			696.3	714.5	1180.8	1193.3	913

**Table S17.** Energy content data for salts 10-16.

Salt No.	Anion	2 X Cation	$\text{HOF}_{\text{cation}}$ (kJ/mol)	$\text{HOF}_{\text{anion}}$ (kJ/mol)	$U_{\text{POT}}$ (kJ/mol)	$H_L$ (kJ/mol)	$\text{HOF}_{\text{salt}}$ (kJ/mol)
10			634.8	344.6	1333.2	1345.6	268
11			761.2	344.6	1258.7	1271.1	596

12			674.2	344.6	1258.7	1271.1	421
13			753.8	344.6	1120.9	1133.3	719
14			796.4	344.6	1144.8	1157.2	779
15			668.4	344.6	1133.7	1146.1	535
16			1112.0	344.6	1044.0	1056.4	1512

## References

1. Arulsamy, N.; Bohle, D. S.; Doletski, B. G. *Inorg. Chem.* **1999**, *38*, 2709-2715.
2. Westwell, M. S.; Searle, M. S.; Wales, D. J.; Williams, D. H. *J. Am. Chem. Soc.* **1995**, *117*, 5013-5015.
3. Gaussian 09, Revision E.01, M. J. Frisch, G. W. Trucks, H. B. Schlegel, G. E. Scuseria, M. A. Robb, J. R. Cheeseman, G. Scalmani, V. Barone, B. Mennucci, G. A. Petersson, H. Nakatsuji, M. Caricato, X. Li, H. P. Hratchian, A. F. Izmaylov, J. Bloino, G. Zheng, J. L. Sonnenberg, M. Hada, M. Ehara, K. Toyota, R. Fukuda, J. Hasegawa, M. Ishida, T. Nakajima, Y. Honda, O. Kitao, H. Nakai, T. Vreven, Jr. J. A. Montgomery, J. E. Peralta, F. Ogliaro, M. Bearpark, J. J. Heyd, E. Brothers, K. N. Kudin, V. N. Staroverov, R. Kobayashi, J. Normand, K. Raghavachari, A. Rendell, J. C. Burant, S. S. Iyengar, J. Tomasi, M. Cossi, N. Rega, J. M. Millam, M. Klene, J. E. Knox, J. B. Cross, V. Bakken, C. Adamo, J. Jaramillo, R. Gomperts, R. E. Stratmann, O. Yazyev, A. J. Austin, R. Cammi, C. Pomelli, J. W. Ochterski, R. L. Martin, K. Morokuma, V. G. Zakrzewski, G. A. Voth, P. Salvador, J. J. Dannenberg, S.

Dapprich, A. D. Daniels, O. Farkas, J. B. Foresman, J. V. Ortiz, J. Cioslowski, D. J. Fox, *Gaussian*, Inc., Wallingford CT, **2013**.

4. Politzer P, Ma Y, Lane P, Concha MC (2005) Int J Quant Chem 105: 341-347.
5. Lu T, Chen F (2012) *J Comput Chem* 33: 580–592.
6. H. D. B.Jenkins, D. Tudela, L. Glasser, Lattice Potential Energy Estimation for Complex Ionic Salts from Density Measurements, *Inorg. Chem.* **2002**, *41*, 2364.